

## **Coupling Infrastructure Resilience and Flood Risk Assessment via Copulas Analyses for a Coastal Green-Grey-Blue Drainage System under Extreme Weather Events**

Justin Joyce<sup>1</sup>, Ni-Bin Chang<sup>1</sup>, Rahim Harji<sup>2</sup> and Thomas Ruppert<sup>3</sup>

<sup>1</sup>Department of Civil, Environmental, and Construction Engineering Department, University of Central Florida, Orlando, FL, USA <sup>2</sup>Watershed Management Section, Pinellas County Government, Largo, FL, USA <sup>3</sup>Florida Sea Grant College Program, Miami, FL, USA

### **Abstract**

This study sheds light on the coupling of potential flood risk and drainage infrastructure resilience of low-lying areas of a coastal urban watershed to evaluate flood hazards and their possible driving forces. Copulas analyses with the aid of joint probability of simultaneous occurrence help characterize the complexity for hazard classification based on subsequent exposure to inundation under varying levels of adaptive capacity. Adaptive measures of consideration include traditional flood proofing structures and low impact development facilities for a coastal urban watershed - the Cross Bayou watershed, near Tampa Bay, Florida. Findings indicate that coupling flood risk and infrastructure resilience is achievable by the careful formulation of flood risk associated with a resilience metric, which is a function of the predicted hazards, vulnerability, and adaptive capacity. The results also give insights into improving existing methodologies for municipalities in flood management practices such as incorporating a multi-criteria flood impact assessment that couples risk and resilience in a common evaluation framework.

Keywords: flood impact, risk analysis, resilience assessment, coastal sustainability

### **Software Availability**

Name of software: Interconnected Channel and Pond Routing (ICPR) version 4

Developers: Streamline Technologies, Inc.

Hardware required: 8 GB of Ram or higher, Intel Core i5 processor or higher

Operating system required: Microsoft Windows

Availability: Contact Streamline Technologies, Inc. 1900 Town Plaza Court, Winter Springs, Florida, 32708 or by email [sales@streamnologies.com](mailto:sales@streamnologies.com)

Name of Software: MATLAB

Developers: Math Works

Hardware required: 1 GB of GPU memory or more

Operating System Required: Windows, Mac or Linux

Availability: Contact MathWorks [https://www.mathworks.com/company/aboutus/contact\\_us/contact\\_sales.html](https://www.mathworks.com/company/aboutus/contact_us/contact_sales.html)

Code/Scripts: Contact University of Central Florida (UCF) Stormwater Academy for MATLAB Script of Copula Analyses

## **INTRODUCTION**

### ***Background***

In May 2015, the Florida Legislature passed and the Governor signed into law SB 1094 [<https://www.flsenate.gov/Session/Bill/2015/1094>] which regards the consideration of future flood impacts in Florida Comprehensive Plans, particularly from a coastal management perspective. These new requirements, which concern development and redevelopment efforts to reduce the flood risk, include natural hazards such as high tide events and sea level rise. Risk in this context can be described as the likelihood of a flood hazard occurring with an associated loss or negative impact. The likelihood of associated loss or negative impact is dependent on several factors, such as the flood hazard considered and the level of vulnerability to flooding. The concepts of hazard and vulnerability can be thought of as the physical manifestations or occurrences of adverse events and the propensity or predisposition to be adversely affected or susceptible to harm (IPCC, 2014), respectively, both of which influence flood exposure simultaneously. Flood exposure is dependent upon the spread of hazardous effects given the vulnerability such as proximity to waterbodies and/or condition of drainage outfalls. The level of risk, however, can be influenced by the level of resilience through the connection to the adaptive capacity in a region such as a low-lying coastal area. The concept of resilience has expanded from its origins in material science and engineering to ecological resilience (Holling, 1973) and eventually to other disciplines such as the social sciences (social resilience) and psychology (psychological resilience). When considering infrastructure systems, such as drainage under flooding, engineering resilience, which is highlighted in this study, is the ability

of such systems to absorb disturbance (i.e., flooding) and recover after a disturbance has occurred, or the ability to continue functionality under adverse conditions (Omer, 2013). While resilience is typically seen as an outcome, it should be viewed as a process which involves adaptation, anticipation, and improvement in basic functions of a considered system (Bahadur et al., 2010).

Coupling flood risk and engineering resilience is by no means an easy task. DeBruijn (2005) defined resilience, in terms of flood risk management, as the ability of a system to recover from floods. Quantitatively, this can be represented via several indicators such as the amplitude or magnitude of the reaction to disturbances, the graduality of reaction(s) under increasing disturbances, and recovery rate (DeBruijn, 2005). A resilient system results in a lower amplitude of reaction to disturbances, low graduality of reaction to increasing disturbances, and a higher recovery rate. Analogously this can be tied to three types of capacity of resilience, proposed by Francis and Bekera (2014), which include absorptive capacity, adaptive capacity, and restorative capacity. The absorptive capacity allows for adequate buffering to absorb or contain hazard effects while adaptive capacity is the ability to adjust or provide the necessary changes in response to adverse impacts such as when absorptive capacity has been exceeded. Restorative capacity is the ability to return to normal function or improved level of performance after a disturbance.

As with many systems, however, the absorptive capacity can fluctuate with changes in hazards, as is the case when considering future flood risk. With this considered, adaptive capacity can be seen as a “bridge” to restorative capacity and eventually resilience when absorptive capacity has been exceeded. Adaptive capacity can be understood as the capacity to cope and adapt to adverse effects or, from a systems approach, the extent to which a system can modify its circumstances to move to a less vulnerable condition (Luers et al., 2003). Adaptive capacity also encompasses the ability to plan, prepare for, facilitate, and implement adaptation options (Klein et al., 2003), which first depend upon the nature of the disturbances or potential disturbances. Subsequently, additional factors such as scale of adaptation (individual to systemic), policy, and constraints must also be considered. Klein et al. (2003) has argued for the use of adaptive capacity as an umbrella concept that includes the ability to prepare and plan for hazards, as well as to implement technical measures before, during, and after a hazard event. All

the while, the strategy for adaptive capacity must be flexible with respect to both risk and resilience (DeBruijn, 2005) in order to reduce rigidity in case of disruptive events (Park et al., 2013).

While absorptive capacity can provide an “initial gauge” of resilience, when exceeded failure is imminent unless adaptive measures are taken. This is particularly concerning for system design based upon a particular risk event as opposed to system design adaptive to various levels of risk. Essentially, as Park et al. (2013) argued, the risk-based approach considers developing resistance to identified threats as opposed to resilience-based approaches which embrace uncertainty and failure due to possible threats via anticipation and adaptation. However, in this regard, risk and resilience cannot be applied individually but must work together. Risk provides a starting point for identifying potential problems or threats at hand; however, resilience considers how the progression can be maintained in the face of potential problems or threats.

### ***Review of Methods***

When considering flooding in risk analysis and resilience assessment in particular, flooding can be caused by any combination of hazards, the combination of which would impact both risk and resilience. This is particularly important for coastal communities, which typically are low-lying and can face heavy rainfall, high tide events, and sea level rise within the same time period. Subsequently, there exists a level of uncertainty of any combination of hazards occurring with corresponding consequence(s). Joint probability analysis is useful in this regard for determining the probability of potential flooding hazards occurring simultaneously rather than in isolation. A univariate analysis alone cannot provide a complete assessment of the occurrence probability of potential flooding hazards or scenarios, particularly if they are interdependent (Chebana and Ouarda, 2011). However, with typical multivariate analyses, one condition is for the variables in question to be independent from one another (Wahl et. al, 2012). A univariate analysis also lacks consideration of flooding under multivariate hazards, particularly for coastal communities, when worst case flooding can occur under combined heavy rainfall and high tide events (Xu et. al, 2014). The choice of multivariate analysis must take into consideration that the variables in question could be interdependent, may not be under the same family of marginal distributions, and are not normally distributed.

Both Bayesian networks and copulas have been utilized for analyzing multivariate problems (Cleophas, T.J. and Zwinderman, 2013; Nelson, 2006). However, Bayesian networks require the need for prior information or knowledge for defining conditional probability distributions and the structure of the network. Depending on the level of detail needed to build such networks, the computational demand can be quite large (Unsitalo, 2007) compared to copulas. For this reason, copulas can be particularly useful. While copulas have wide applications across several disciplines such as finance and insurance, the applications of copulas within hydrology in particular is important since hydrological processes are typically multidimensional in nature and indicate certain levels of interdependence (De Michele et al., 2007). Several applications of copulas in hydrology (Table 1) consisted of analyzing the joint behavior of several hydrological variables during storm events while capturing important statistical dependences (De Michele and Salvadori 2003; Salvadori and De Michele 2004; Balistrocchi and Bacchi, 2011), modeling of multivariate hydrological extremes (Favre et al., 2004; Zhang et al., 2011), rainfall frequency analysis (Zhang and Singh, 2007), flood frequency analysis (Wang et al., 2009) and hydraulic structural design for flooding (De Michele et al., 2005). Particularly for inland coastal areas, copulas have been useful in analyzing coastal hazards (Table 2) with underlying hydrological and hydrodynamic processes (De Michele et al., 2007; Wahl et al., 2012; Corbella and Stretch, 2013; Xu et al., 2014; Trepanier et al., 2014).

**Table 1: Applications of Copulas for Varying Hydrology Topics**

<b>Topic of Concerns</b>	<b>Copula Variables</b>	<b>References</b>
• Rainfall Characteristics	<ul style="list-style-type: none"> <li>• Storm intensity and duration<sup>1</sup></li> <li>• Rainfall volume and duration<sup>2</sup></li> </ul>	<ul style="list-style-type: none"> <li>• De Michele and Salvadori (2003)<sup>1</sup></li> <li>• Salvadori and De Michele (2004)<sup>1</sup></li> <li>• Balistrocchi and Bacchi, (2011)<sup>2</sup></li> </ul>
• Extremes	• Peak flows and volumes	• Favre et al. (2004)
• Rainfall Frequency Analysis	<ul style="list-style-type: none"> <li>• Rainfall duration and intensity</li> <li>• Rainfall depth and intensity</li> </ul>	• Zhang and Singh (2007)

	• Rainfall duration and depth	
• Flood Frequency Analysis	• Peak flow (confluence)	• Wang, Chang, and Yeh (2009)
• Structural Design (Flood Risk)	• Flood peak and volume	• De Michele et al. (2005)

Note: The superscripts in the second and the third columns link the respective copula variables in the second with their respective references in the third column.

**Table 2: Applications of Copulas for Coastal Areas**

<b>Hazard</b>	<b>Copula Variables</b>	<b>References</b>
• Sea Storm	• Significant wave height, storm duration, storm direction, and storm inter-arrival time <sup>1</sup> • Wave height, wave period and storm duration <sup>2</sup>	• De Michele et al. (2007) <sup>1</sup> • Corbella and Stretch (2013) <sup>2</sup>
• Storm Surge	• Highest turning point, intensity and significant wave height	• Wahl et al. (2012)
• Extreme Rainfall • Storm Tide	• Annual peak 24-hr rainfall and tide level	• Xu et al. (2014)
• Tropical Cyclones	• Storm surge height and wind speed	• Trepanier et al. (2014)

Note: The superscripts in the second and the third columns link the respective copula variables in the second with their respective references in the third column.

As shown in the previously listed studies, copulas can be used to highlight interdependence and the multi-dimensional nature of flooding and climate processes, however, they highlight only one aspect of overall flood risk. Without considering resilience to these interdependent and multi-dimensional events, overall flood risk cannot be assessed. Quantifying

flood resilience depends on the interconnection of the urban space and the natural space. This interconnection can be represented by the concept of networked systems or networked infrastructure systems when considering infrastructure (Omer, 2013). With regard to flood risk and resilience, natural and man-made systems such as rivers, canals, stormwater drainage channels, and pipes are seen as the first system(s) that natural flooding hazards interact with before effects are felt within surrounding systems, such as residential communities, given the level of resilience of such systems. As a result, the adaptive capacity of natural and man-made systems become important to the overall flood risk and resilience due to the “cascade effect” of interconnected systems (Omer, 2013; Park et al., 2013).

A useful real-world example for consideration of both flood risk and infrastructure resilience is the Cross Bayou Watershed, located within Pinellas County near the Tampa Bay region of West-Central Florida. Low lying areas within the Cross Bayou Watershed have been historically prone to flooding driven by rainfall runoff and/or high tide events. Over the years, storm events and subsequent flooding have taken a toll on the drainage infrastructure, particularly for the undersized conveyance systems found throughout the watershed which are not equipped to handle increased runoff from surrounding urbanization. Tidal flooding has also impacted low-lying areas near a tidal canal which dissects the watershed connecting neighboring bays for which inadequate protection exists. Water within the canal can flow in either direction depending upon tidal conditions. Flooding occurs periodically in several low-lying communities with strong interactions between the surface water and the groundwater systems. In dealing with such a complex system, the Interconnected Pond and Channel Routing (ICPR) catchment model (Streamline Technologies Inc., 2015) was applied to the study region for coupling risk and resilience in support of multi-criteria flood impact assessment. The objectives of this study are to: (1) determine the dependence structure of potential flooding risk in a low-lying area within the Cross Bayou Watershed via a copulas analysis, (2) link flood risk and engineering resilience via implementing a risk formulation which includes a resilience metric that is dependent upon the hazard, vulnerability, and exposure of an area of concern, and 3) conduct a multi-criteria flood impact assessment for decision analysis. Such efforts may answer the following scientific questions: 1) can the copulas analysis fully support the risk analysis? 2) how can potential flood risk be offset by modeling adaptive measures for increasing drainage infrastructure resilience

with the aid of ICPR? and 3) can the well coupled flood risk and engineering resilience lead to better decision making via a multi-criteria flood impact assessment? Results of this study will have implications for policy makers such as those in Pinellas County who are seeking new ways of reducing the flood insurance rates of their constituents by considering new flood management strategies. This paper serves as a companion study of Joyce et al. (2017).

## **STUDY AREA**

The Cross Bayou Watershed of Pinellas County (Figure 1), Florida, was selected as a case study because of its vulnerability to coastal flooding and Pinellas County's efforts to implement improved stormwater management to increase the area's adaptive capacity to future hazards. The Cross Bayou watershed encompasses approximately 31 km<sup>2</sup> (7,697 acres), primarily comprised of high-density residential, industrial, and commercial areas. An important feature of the watershed is a 16.9 km (10.5-mile) long constructed tidal canal, the Cross Bayou Canal (Figure 1), which dissects the watershed and connects Tampa Bay and Boca Ciega Bay on its northeastern and southwestern ends, respectively. The Cross Bayou Canal also intersects the Pinebrook Canal to the southwest (Figure 1). Water within the canal can flow in either direction, depending on tidal conditions. This feature, while useful for overall watershed drainage, is potentially hazardous to low-lying communities during high tide events, particularly when considering the ongoing threat of sea level rise (NOAA, 2016) near the Tampa Bay region.



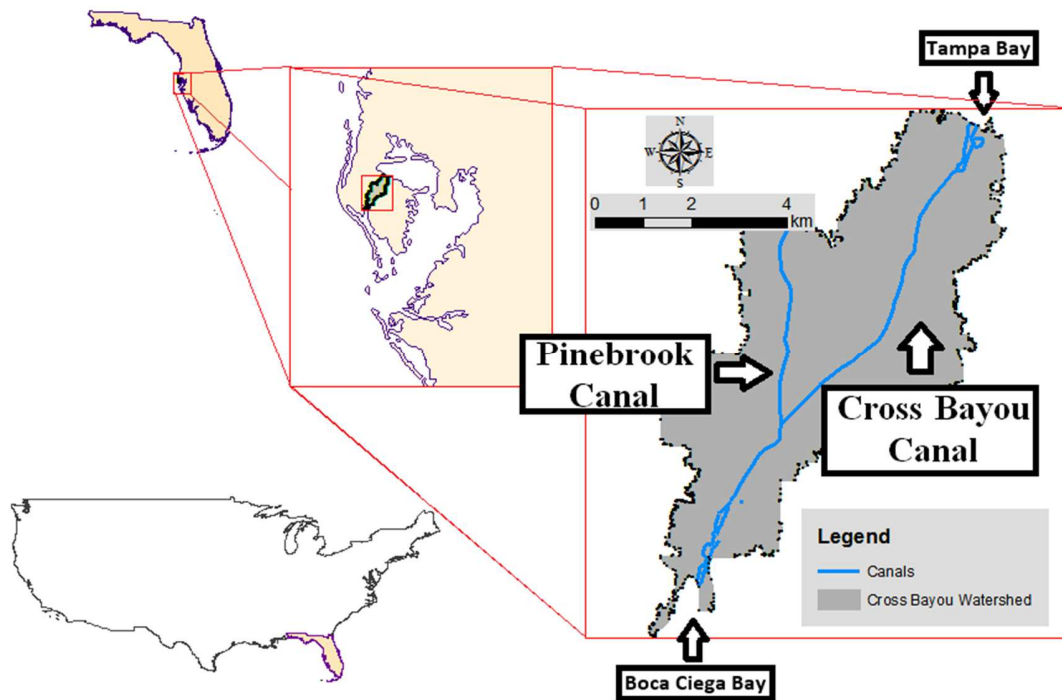


**Fig.1: Extent of Cross Bayou Watershed**

Some areas in the watershed are consistently more vulnerable and have a decreased adaptive capacity to flooding. The Mariners Cove residential community (Figure 2), in particular, is known for significant flooding from storm events. Flooding in the Mariners Cove community is primarily caused by heavy rains and high tide events of the adjacent Cross Bayou canal.

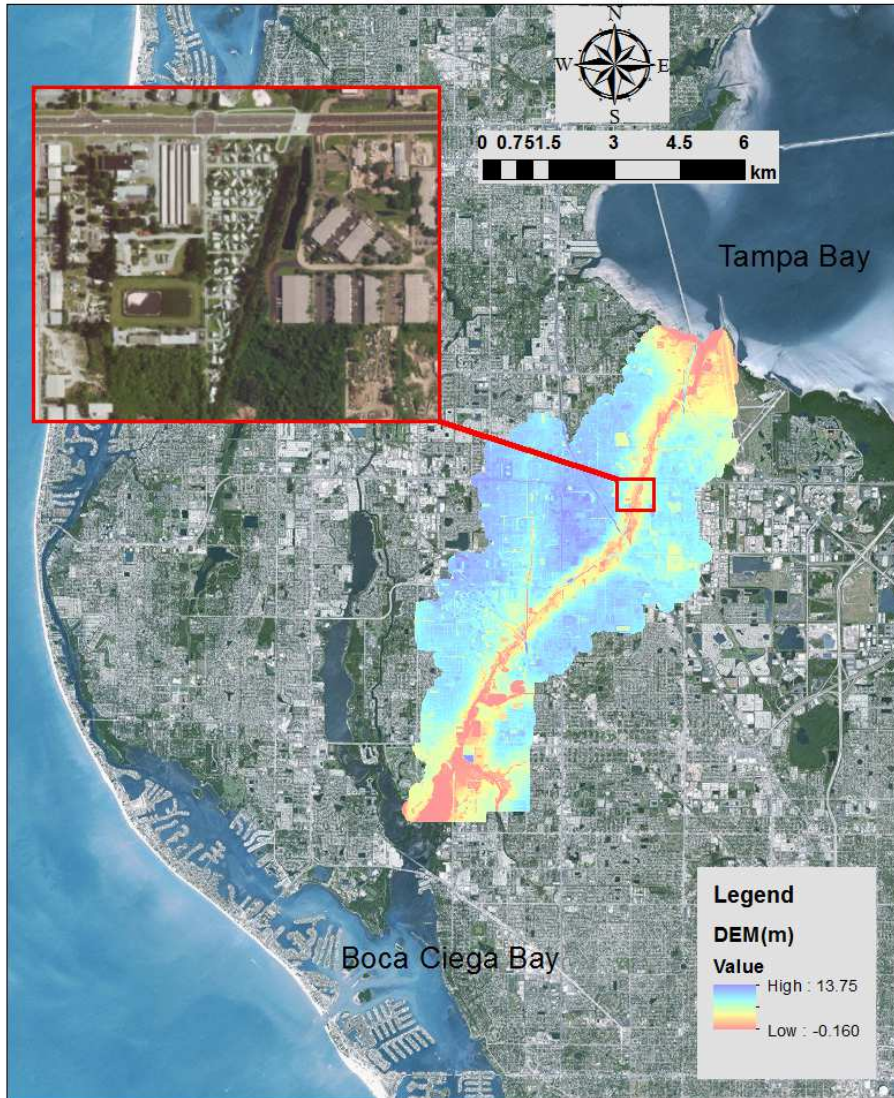


**Fig.2: Extent of example low-lying community (the Mariners Cove area) in Cross Bayou Watershed vulnerable to coastal flood hazards. Source of Satellite Imagery: Esri, DigitalGlobe, GeoEye, Earthstar Geographics, CNES/Airbus DS, USDA, USGS, AeroGRID, IGN and GIS User Community**

## METHODOLOGY

There are many relevant definitions of risk and resilience in the literature. The methods outlined in this section focus on the essence of rational choice and the actualization for coupling of risk and resilience.

***Risk Formulation***

Risk, in a generalized formulation, can be represented as follows:

$$\text{Risk} = f(\text{likelihood or probability of consequences occurring and consequences}) \quad (1)$$

Risk as a function of likelihood of consequences is related to decision theory such that risk can be represented as an expected value as follows:

$$\text{Risk (Expected Value)} = \text{likelihood or probability of consequences occurring} \times \text{consequences} \quad (2)$$

$$\text{Likelihood or probability of consequences occurring} = f(\text{Hazard, Vulnerability, Resilience}) \quad (3)$$

$$\text{Consequences} = f(\text{Exposure}) = f(\text{Hazard, Vulnerability}) \quad (4)$$

The likelihood or probability of consequences occurring is a function of hazard, vulnerability, and resilience. The consequences are a function of exposure, which is also a function of hazard and vulnerability. Literature can provide some guidance with regard to how the elements of hazard, vulnerability, resilience and exposure are related mathematically. Table 3 details the essence of this issue in an attempt to provide a mathematical formulation of risk. .

**Table 3. Variations in the risk formulation in literature**

Risk Formulation	Source
<del>Risk=Hazard</del> × Vulnerability	<ul style="list-style-type: none"> <li>▪ Ciurean, Schroter and Glade (2013)</li> <li>▪ UN International Strategy for Disaster Reduction (UNIDSR,</li> </ul>

	2002)
$\frac{\text{Hazard} \times \text{Vulnerability}}{\text{Adaptive Capacity}}$	<ul style="list-style-type: none"> <li>▪ Food and Agriculture Organization (2003)</li> <li>▪ World Health Organization(2007)</li> </ul>
$\text{Risk}=\text{Hazard} \times (\text{Exposure} \times \text{Sensitivity} \times \text{Resilience})$	<ul style="list-style-type: none"> <li>▪ Johansen (2010)</li> </ul>

In the aforementioned risk formulations, sensitivity is the degradation in performance during continuous effects from hazards from a physical system perspective (Johansen, 2010). Aside from the generalized formulations presented in Table 3, mathematically, the formulations have advantages and disadvantages and will be presented on a case by case basis below:

**Case I:** 
$$\text{Risk}=\text{Hazard} \times \text{Vulnerability} \tag{5}$$

For this case, the risk formulation is general and not specific in scope such that the application of this risk formulation assumes that hazard and vulnerability are only considered without other elements such as exposure or resilience unless defined further by the user of such formulation.

**Case II:** 
$$\text{Risk}=\text{Hazard} \times (\text{Exposure} \times \text{Sensitivity} \times \text{Resilience}) \tag{6}$$

For this case, the risk formulation is expounded upon by breaking down the vulnerability term as a product of exposure, sensitivity, and resilience. This formulation is less simplistic than in Case I. However, this formulation can only be applied carefully, depending on how the resilience term is defined.

**Case III:** 
$$\text{Risk} = \frac{\text{Hazard} \times \text{Vulnerability}}{\text{Adaptive Capacity}} \tag{7}$$

Case III applies a quotient. Adaptive capacity is also one aspect of resilience as defined in literature such as Francis and Bekera (2014). However, the quotient term presents challenges given how adaptive capacity is defined or formulated such that adaptive capacity could be large or small. In the case of very small numbers for adaptive capacity, the risk can be considerably large. Conceptually this makes sense, however, quantitatively this presents challenges for interpretation. The success of this formulation depends on how the quotient term, adaptive capacity or resilience, is defined.

### ***Resilience Formulation***

The resilience term, throughout the literature, does not have a consistent form and varies given the system and assumed response. For infrastructure or engineering systems, Yodo and Wang (2016) have outlined how resilience metrics are developed based on three categories or approaches, as summarized in Table 4.

**Table 4. Framework for Defining Engineering/Infrastructure Resilience Metrics as Adapted from Yodo and Wang (2016)**

Category/Approach	Based on theoretical resilience curves	Based on pre- and post-disruptions performances	Based on reliability and restoration
<i>Description</i>	Quantitative resilience metric developed from the properties of theoretical resilience curves	Quantitative resilience metrics developed from system performance before (pre-) and after (post-) disruption	Quantifies resilience from a system's ability to maintain its capacity and performance during a given period of time and to restore its capacity and performance

With respect to the first category/approach from Table 4, defining a quantitative resilience metric based on theoretical resilience curves may present problems since resilience curves could be non-linear in form and may not follow a defined pattern given variation in hazard or disruption. Defining a quantitative resilience metric based on (1) pre- and post-disruptions performances and (2) reliability and restoration may be more useful for this study. Francis and Bekera (2014) proposed a resilience metric that can account for both pre- and post-disruptions along with reliability and restoration in the following formulation:

$$\text{Resilience} = S_p \times \left( \frac{F_r}{F_o} \right) \times \left( \frac{F_d}{F_o} \right) \quad (8)$$

where  $S_p = \text{speed recovery factor} = \left\{ \begin{array}{l} \left( \frac{t_\delta}{t_r^*} \right) e^{[-a(t_r - t_r^*)]} \text{ for } t_r \geq t_r^* \\ \left( \frac{t_\delta}{t_r^*} \right) \text{ otherwise} \end{array} \right\}$

$F_r$  = system recovery state

$F_o$  = original system state

$F_d$  = system state following disruption

$\left( \frac{F_r}{F_o} \right)$  = adaptive capacity

$\left( \frac{F_d}{F_o} \right)$  = absorptive capacity

$t_\delta$  = slack time or the max time during post-disruption that is accepted before recovery begins

$t_r$  = time to final recovery (i.e. new equilibrium state)

$t_r^*$  = time to complete initial recovery actions

$a$  = decay in resilience parameter representing time to new equilibrium state

From the aforementioned resilience metric, the decay factor,  $a$ , is represented such that if the initial recovery takes longer than the slack time the resilience metric decreases. However, this metric, as proposed by Francis and Bekera (2014) presented a challenge regarding what value to assign the decay parameter. In addition, the slack time variable is subjective depending on the system of concern and decision maker. Lastly, when considering flooding, the variable

representing the original system state,  $F_o$  would be assumed zero since the system (i.e., drainage) is at a dormant or no activity state, resulting in the ratio becoming undefined.

In this specific case, a potentially useful metric should be modified by considering the difference between the initial recovery time (i.e., initial reduction in inundation depth after maximum inundation area) and the final recovery time (i.e., no inundation or no exposure):

$$\text{Relative Change in Time of Exposure} = \frac{T_f - T_i}{T_i} \quad (9)$$

$T_i$  = initial recovery time (time in which inundation depths are initially reduced from maximum inundation depths, i.e. max exposure)

$T_f$  = final recovery time (time in which inundation depths are non-existent following maximum inundation depths, i.e. max exposure)

A resilience metric can be created that is the reciprocal of the relative change in time of exposure and is represented as follows:

$$\text{Resilience} = \frac{1}{\left[ \frac{T_f - T_i}{T_i} \right]} \quad (10)$$

Visually, the resilience term can be represented by Figure 3. The goal of the resilience metric is to minimize the difference in the numerator ( $T_f - T_i$ ) such that the system in question can achieve recovery in a shorter period of time (i.e.  $T_f - T_i$  is small in value). Achieving shorter recovery times highlights greater resilience such that, when considering concepts proposed by Francis and Bekera (2014), absorptive capacity, adaptive capacity and restorative capacity of the system are greater. The goal subsequently would be to implement a system that achieves greater absorptive capacity, adaptive capacity, and restorative capacity.

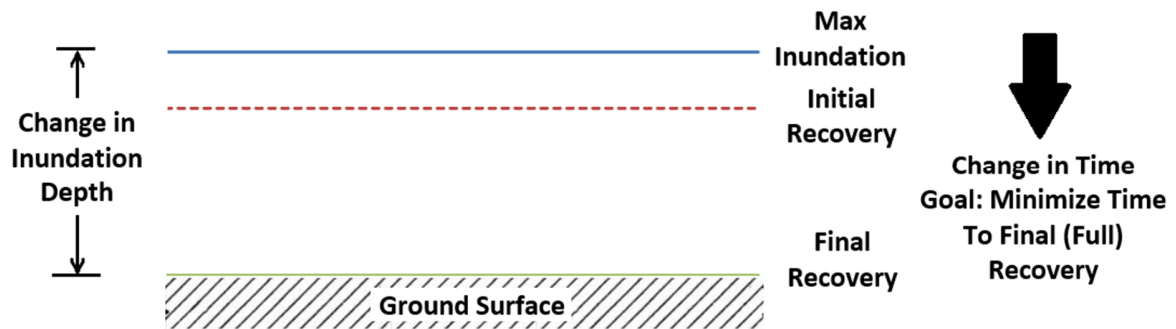


**Fig. 3: Schematic of determining the resilience metric**

***The Proposed Risk Formulation & Framework***

Given the proposed resilience metric, the Case III risk formulation is more appropriate to utilize in this study and can be represented in the following generalized formulation:

$$\text{Risk} = \frac{\text{Hazard} \times \text{Vulnerability} \times \text{Exposure}}{\text{Resilience}} \tag{11}$$

1. **Risk** = Expected value of negative impact given the product of hazard, vulnerability, exposure, and resilience components. Increases in hazard, vulnerability and exposure could increase risk; however, by minimizing the overall recovery time, represented by the resilience metric, risk can be reduced.



$$\text{Risk} = \frac{\left[ \underbrace{\prod \text{Hazard Weight} \times \prod \text{Vulnerability Weight}}_{\text{Likelihood}} \times \underbrace{\text{Exposure Weight}}_{\text{Consequences}} \right]}{\text{Resilience}} \quad (12)$$

**2. Hazard**= Product of joint probabilities of combinations of variables that could contribute to flood hazard via normalized Archimedean copula PDF plots (see Appendix B).

**3. Vulnerability** = Product of applied weights, normalized between 0 and 1 with 1 being the highest, to a given area of concern based upon several factors such as elevation, distance to waterbodies, and drainage capacity.

**4. Exposure** = Inundation depth value for an area of concern, normalized from 0 to 1.

**5. Resilience**

$$\text{Resilience} = \frac{1}{\left[ \frac{T_f - T_i}{T_i} \right]}$$

$T_i$  = initial recovery time (time in which inundation depths are initially reduced from maximum inundation depths, i.e. max exposure)

$T_f$  = final recovery time (time in which inundation depths are non-existent following maximum inundation depths, i.e. max exposure)

Minimizing the difference between the initial recovery time  $T_i$  and the final recovery time [i.e., the numerator  $(T_f - T_i)$ ] results in reduction of risk due to faster recovery.

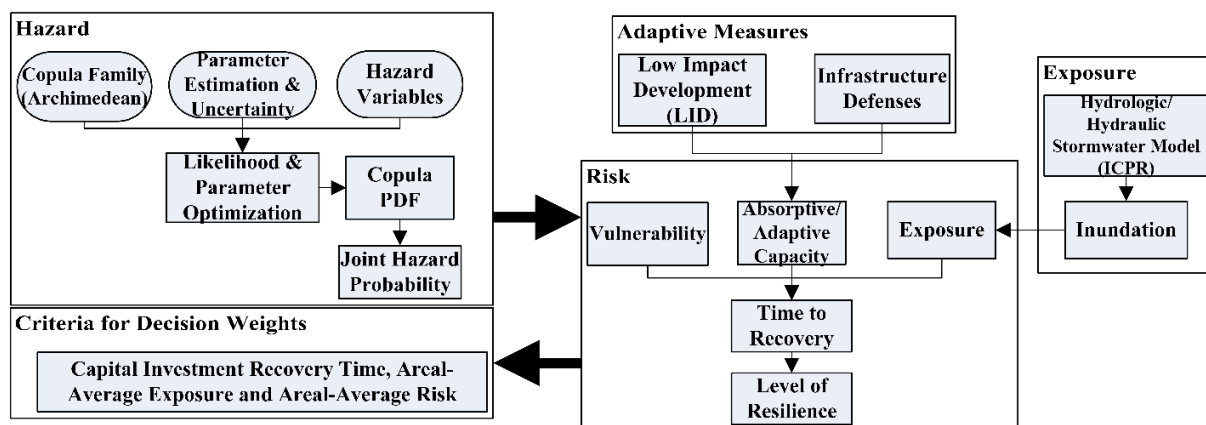


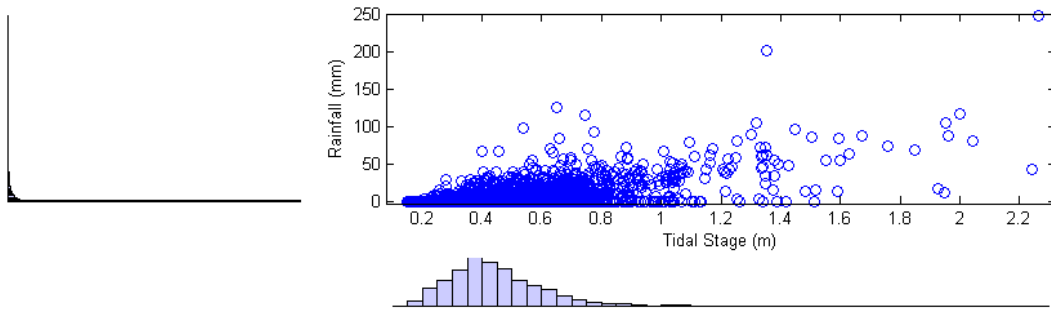
**Fig.4: Methodology framework**

### ***Hazard Variables***

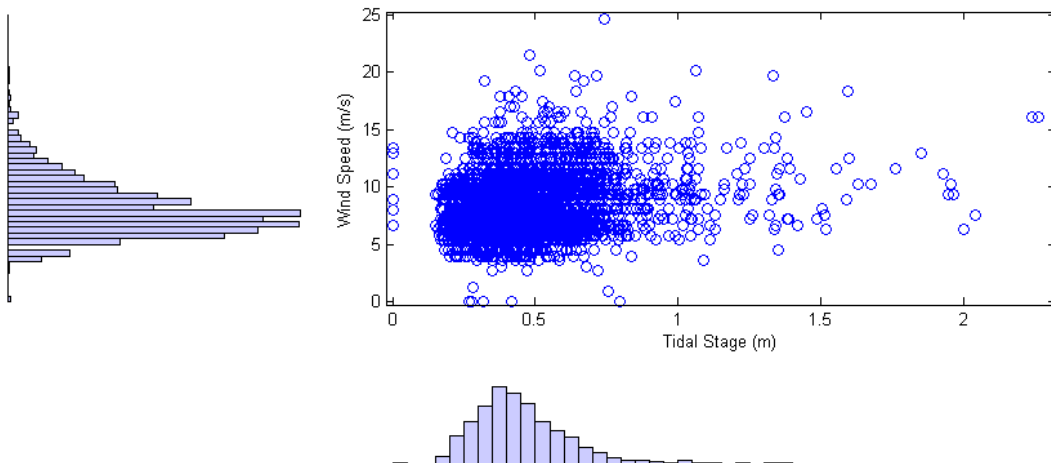
Copulas have emerged, particularly in hydrology, as a useful approach for analyzing multivariate processes or events such as floods. For low-lying coastal areas in particular, such as the Cross Bayou Watershed, flooding can occur in two cases: (1) with respect to storm tide and/or rainfall from a tropical storm event or (2) high tide and/or rainfall from a non-tropical storm event. Flooding does not occur in isolation and is dependent on several variables within nature. In this study, the potential interdependence of daily stage levels in the Cross Bayou Canal, daily rainfall, daily average wind speed, daily barometric pressure and moon phasing (fraction of moon illumination) (Figure 5) from observed stations (Figure 6) are sought to characterize flood hazard potential.

Tidal stage within the canal could be potentially affected by factors such as the following: (1) rainfall runoff which drains into the canal from upstream areas, (2) high winds from tropical storms which can contribute to storm surges, (3) barometric pressure which could increase tidal stage with decreasing pressure, and (4) moon phasing such that tides can rise higher and fall lower during new and full moons (fraction of moon illumination values of 0 and 1 respectively) while rising and falling moderately during first and third-quarter moon phases (values near 0.25 and 0.75, respectively). As evident in Figure 5, weak to no correlation is present between the following: (c) tidal stage and wind direction, (d) tidal stage and barometric pressure and (e) tidal stage and fraction of moon illumination. These combinations will not be evaluated by the

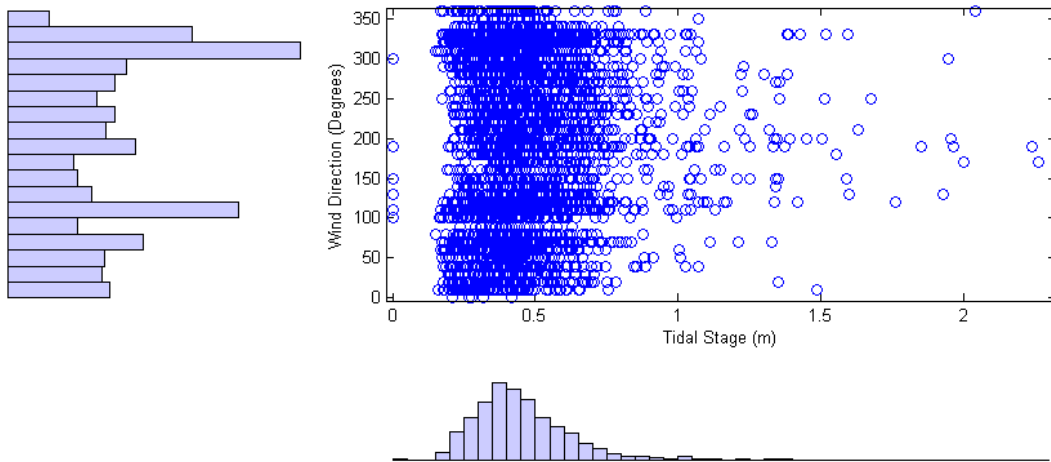
proposed copula analyses in this study. Since wave height is not continuous for the same period of record as rainfall and wind speed, wave height will be the limiting factor for the period of analysis. The year 2012, however, is a worthwhile period for copula analysis with associated daily rainfall and daily tidal stage at their maximums during the year 2012 compared to the entire period of record 2002-2014. Wave height data is also available for the year 2012.



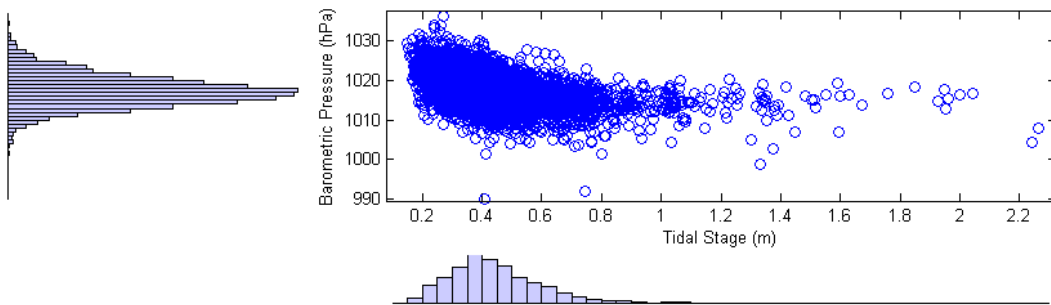
(a)



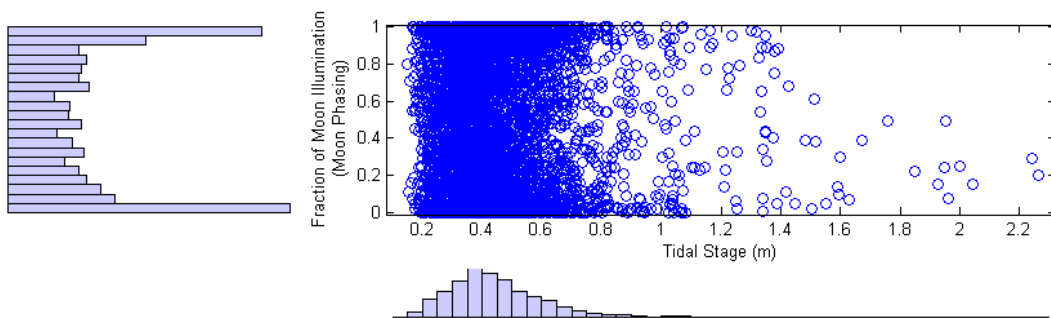
(b)



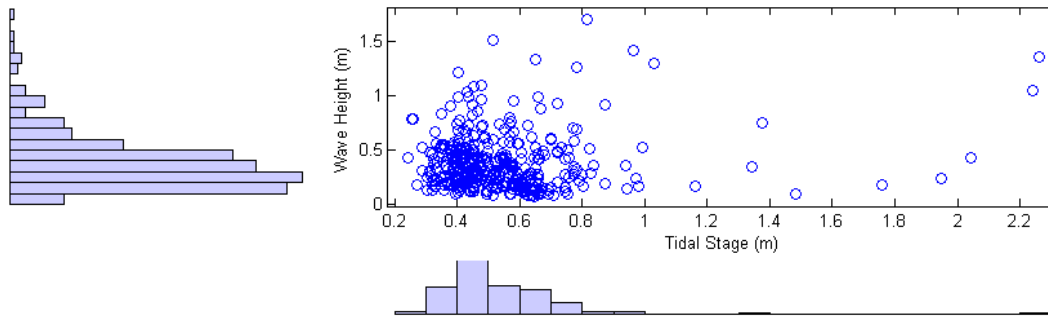
(c)



(d)



(e)



(f)

**Fig.5: Relationship between (a) tidal stage and rainfall (b) tidal stage and fastest 2-minute wind speed, (c) tidal stage and wind direction for fastest 2-minute wind speed, (d) tidal stage and barometric pressure and (e) tidal stage and moon phasing for a continuous period of record (7/30/2002-12/31/2014). For the year 2012, relationship between (f) wave height and tidal stage.**

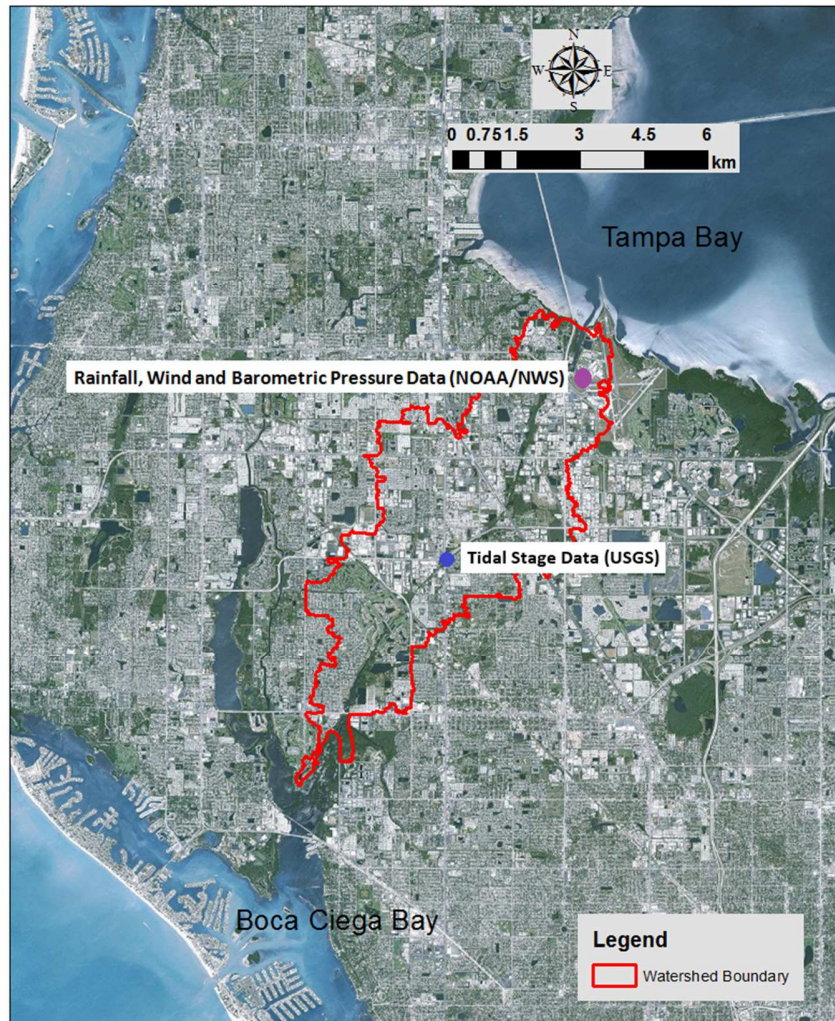


**Fig. 6: Locations of tidal stage, rainfall, wind speed and barometric pressure data for copula analysis. Note: Wave Height Data was obtained from an offshore buoy (27°20'29" N 84°16'20" W) managed by the NOAA National Data Buoy Center. A fraction of Moon Illumination data was obtained from the Astronomical Applications Department of the U.S. Naval Observatory. Note: NOAA is the National Oceanic Atmospheric Administration, NWS is the National Weather Service and USGS is the United States Geological Survey. Source of Satellite Imagery: Esri, DigitalGlobe, GeoEye, Earthstar Geographics, CNES/Airbus DS, USDA, USGS, AeroGRID, IGN and GIS User Community**

*Copula Functions*

The copula has its origins in Sklar's theorem (Nelsen, 2006), which states that given a joint distribution function,  $H$ , with marginal distributions  $F_1$  and  $F_2$ , there exists a copula function  $C$  for all real values of  $x$  and  $y$ :

$$H(x, y) = C(F_1(x), F_2(y)) \quad (13)$$

Sklar's theorem can also be applied to  $n$ -dimensions such that with a distribution function  $H$ , of  $n$ -dimensions, with marginal distributions  $F_1, F_2, \dots, F_n$  there exists a copula  $C$  of  $n$ -dimensions for all real values of  $x$ :

$$H(x_1, x_2, \dots, x_n) = C(F_1(x_1), F_2(x_2), \dots, F_n(x_n)) \quad (14)$$

The choice in copula is important based upon its ability to capture the dependency structure of the variables considered. Archimedean copulas are used in a wide range of applications because they are easily constructed (Nelson, 2006) and are capable of capturing wide ranges of dependence. Archimedean copulas include the one-parameter families (Gumbel, 1960; Clayton 1978; Ali, Mikhail and Haq, 1978; Frank, 1979; Joe, 1993) and the bivariate two-parameter BB1-BB3 and BB6-BB9 families (Joe, 1997). An Archimedean copula of  $d$ -dimension(s) can be represented in the following form:

$$C(x_1, \dots, x_d) = \psi[\psi^{-1}(x_1) + \dots + \psi^{-1}(x_d)] \quad (15)$$

where  $\psi$  is a continuous generator function that satisfies the following conditions: (1)  $\psi(1) = 0$ ;

(2)  $\psi(0) = \infty$ ; (3)  $\psi'(t) < 0$  and (4)  $\psi''(t) > 0$  for all values of  $t \in (0, 1]$ . Widely used Archimedean copulas include the Gumbel-Hougaard, Clayton, and Frank copulas. Given  $d$ -dimension(s), the Gumbel- Hougaard copula, Clayton copula, and Frank copula are represented in Table 5.

**Table 5. Archimedean Copulas utilized in this study**

<i>Copula</i>	$C_\theta(x_1, \dots, x_d)$	$\psi(t)$	$\theta$
Gumbel-Hougaard	$\exp\{-[(-\ln F(x_1))^\theta + \dots + (-\ln F(x_d))^\theta]^{1/\theta}\}$	$(-\ln t)^\theta$	$\theta \geq 1$
Clayton	$(F(x_1)^{-\theta} + \dots + F(x_d)^{-\theta} - 1)^{-1/\theta}$	$\frac{t^{-\theta} - 1}{\theta}$	$\theta \geq 0$

Frank	$-\frac{1}{\theta} \ln \left[ 1 + \frac{(e^{-\theta F(x_1)} - 1)(e^{-\theta F(x_2)} - 1) \dots (e^{-\theta F(x_d)} - 1)}{e^\theta - 1} \right]$	$\frac{e^{-\theta} - 1}{e^\theta - 1}$	$\theta \neq 0$
-------	---	--	-----------------

where  $\theta$  is a dependence parameter. The Frank copula allows for both positive and negative dependence while the Gumbel-Hougaard copula allows for more positive dependence and the Clayton copula allows for more negative dependence. However, before the choice in copula can be made for determination of joint hazard probability, a separate methodology (Figure 7) consisting of optimization techniques must be developed. As such, before the identification of the best-fit copula can be made, appropriate parameters must be estimated with a corresponding likelihood value. The best-fitting of the copula is best determined by parameter and likelihood estimation. The ‘‘Maximum Likelihood Estimation’’ method can be utilized as a first step toward determining the best-fit Archimedean copula due to its inherent versatility for varying models and data types (Khadka, 2008). The following steps (Figure 7) are used to outline the determination of maximum log-likelihood using Archimedean copula parameters.

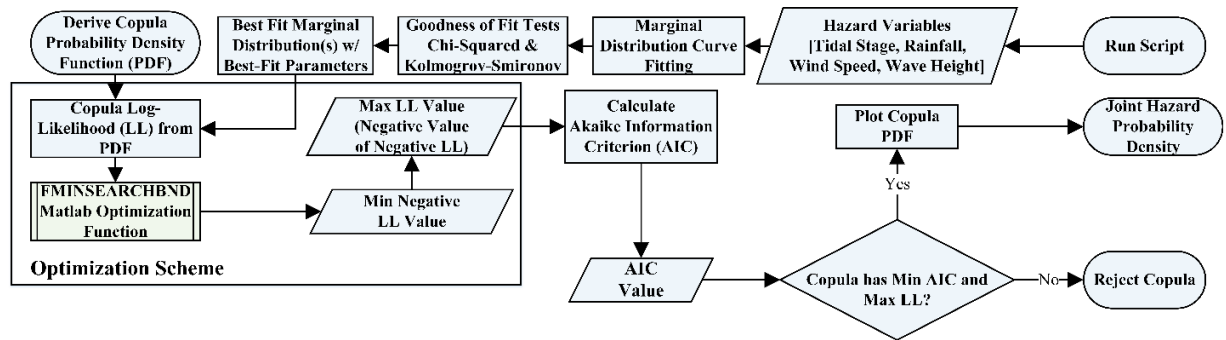


**Fig. 7: Methodology for determination of best-fit Archimedean copula**

1. Given a d-dimensional copula of the form  $C(x_1, \dots, x_d) = \partial F(F_1^{-1}(x_1) \dots F_n^{-1}(x_d))$ , the corresponding copula density function can be expressed as:

$$c(x_1, \dots, x_d) = \frac{\partial^2 C(x_1, \dots, x_d)}{\partial x_1 \dots \partial x_d} = \frac{\partial F(F_1^{-1}(x_1) \dots F_n^{-1}(x_d))}{\partial x_1 \dots \partial x_d} \quad (16)$$

**Table 6. PDFs of Archimedean copulas utilized in this study**

Copula	$C_\theta(x_1, \dots, x_d)$
Gumbel-Hougaard	$\exp\{-[(-\ln F(x_1))^\theta + \dots + (-\ln F(x_d))^\theta]^{1/\theta}\} (F(x_1) \dots F(x_d))^{-1} \left\{ \frac{[(-\ln F(x_1)) \dots (-\ln F(x_d))]^{\theta-1}}{[(-\ln F(x_1))^\theta + \dots + (-\ln F(x_d))^\theta]^{1/\theta}} \right\} \left\{ [(-\ln F(x_1))^\theta + \dots + (-\ln F(x_d))^\theta]^{1/\theta} + \theta - 1 \right\}$



Clayton	$(F(x_1)...F(x_d))^{-\theta-1}(\theta+1)(F(x_1)^{-\theta} + \dots + F(x_d)^{-\theta} - 1)^{\frac{1}{\theta}-2}$
Frank	$\frac{\theta e^{-\theta(F(x_1)+\dots+F(x_d))} (e^{-\theta}-1)}{(e^{-\theta(F(x_1)+\dots+F(x_d))} - e^{-\theta F(x_1)} \dots - e^{-\theta F(x_d)} e^{-\theta})^2}$

2. Assuming parameters for the copula  $C$  and marginal CDFs  $(F_1, \dots, F_d)$  as  $\theta$  and

$\hat{\theta} = [\hat{\theta}_1, \dots, \hat{\theta}_k] = [(\alpha_1, \dots, \alpha_y), \dots, (\alpha_k, \dots, \alpha_y)]$ , respectively, with  $k=1, \dots, d$  where  $d$  represents the number of dimensions and  $y$  is the number of parameters for a respective marginal distribution can be represented by the following density function:

$$f(x_1, \dots, x_d; \theta, \hat{\theta}) = c(F_1(x_1; \hat{\theta}_1), \dots, F_d(x_d; \hat{\theta}_d); \theta) \prod_{k=1}^d f_k(x_k; \hat{\theta}_k) \quad (17)$$

3. Defining a likelihood function  $L: L(\theta; x_i) = \prod_{i=1}^n f(x_i; \theta)$  such that the likelihood of some parameter(s) are a certain value, given the data  $x_1, \dots, x_n$  of  $n$ -observations, is similar to the probability of observing the data given some parameter(s). Given the log-likelihood is

$\ln L(\theta; x_i) = \sum_{i=1}^n \ln f(x_i; \theta)$  the log-likelihood of Eqn. (17), this can be represented as:

$$\begin{aligned} \ln L(\theta, \hat{\theta}; x_1, \dots, x_n) &= \sum_{i=1}^n \ln f(x_{i1}, \dots, x_{id}; \theta, \hat{\theta}) = \\ &= \sum_{i=1}^n c(F_1(x_{i1}; \hat{\theta}_1), \dots, F_d(x_{id}; \hat{\theta}_d); \theta) + \sum_{i=1}^n \sum_{k=1}^d \ln f_k(x_{ik}; \hat{\theta}_k) \end{aligned} \quad (18)$$

for  $k = 1, \dots, d$  where  $d =$  number of dimensions.

4. The negative-log likelihood can be determined by determining the negative of Eqn. (18) as represented:

$$\begin{aligned} -\ln L(\theta, \hat{\theta}; x_1, \dots, x_n) &= -\sum_{i=1}^n \ln f(x_{i1}, \dots, x_{id}; \theta, \hat{\theta}) = \\ &= -\left[ \sum_{i=1}^n c(F_1(x_{i1}; \hat{\theta}_1), \dots, F_d(x_{id}; \hat{\theta}_d); \theta) + \sum_{i=1}^n \sum_{k=1}^d \ln f_k(x_{ik}; \hat{\theta}_k) \right] \end{aligned} \quad (19)$$

with the goal of minimizing the negative log-likelihood which is equivalent to maximizing the log-likelihood. The negative log-likelihood is found using copula-based MATLAB algorithms adapted for Patton (2004) but with changes to account for optimization functions to maximize the log-likelihood.

Once the maximum log-likelihood of each copula, with an associated dependence parameter, is determined (see Appendix B), additional criteria is needed to determine the best-fit copula for the data. The Akaike Information Criterion (AIC) (Akaike, 1974), is typically applied in the selection of semiparametric and parametric copula models, however the Copula Information Criterion has been recently developed to provide criteria for copulas specifically with the drawback of increased computational cost (Jordanger and Tjostheim, 2014). As such, the AIC will be a recommended criterion for this study and is determined as follows:

$$AIC=2K-2\ln(LL) \tag{19}$$

where  $K$  is the number of parameters estimated and  $LL$  is the log-likelihood. Given a set of candidate models for the data, the preferred model is the one with the minimum AIC value for the given maximum likelihood. The AIC value reflects the goodness of fit but it also includes a penalty with each increase in the number of estimated parameters to discourage overfitting.

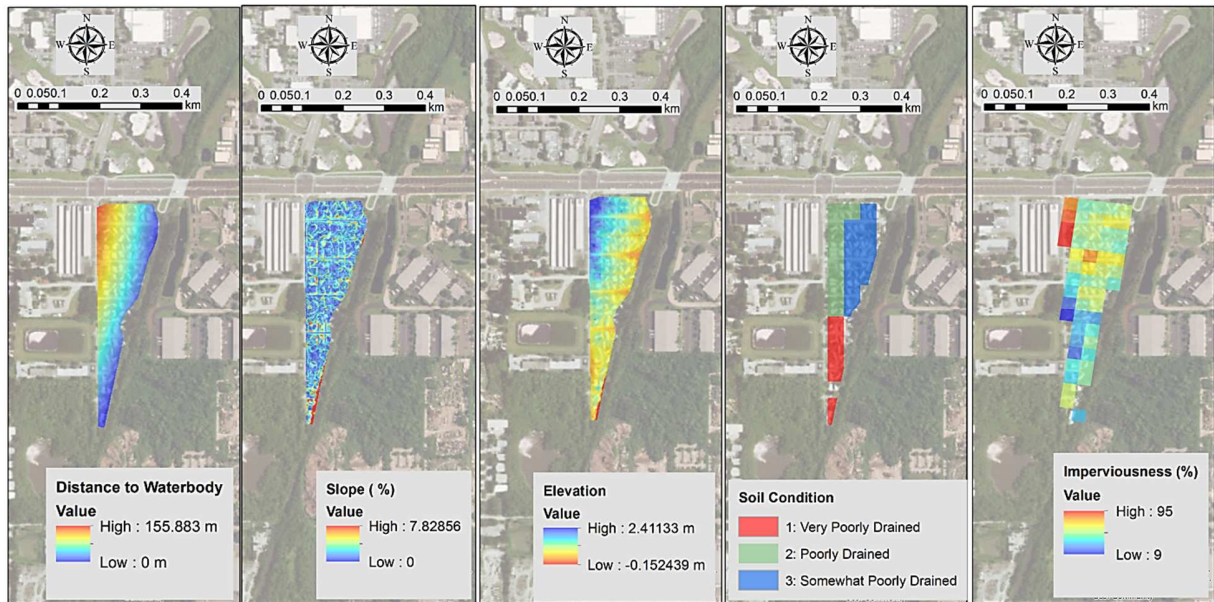
### ***Vulnerability***

The Mariners Cove community was selected as a test site for classifying vulnerability. The vulnerability component of the risk formulation can be quantitatively defined using an applied weighting system based upon the sum of several criteria (Table 7). The criteria are as follows: (1) the distance to a major water body, (2) slope, (3) elevation from a digital elevation map (DEM), (4) soil condition and (5) percent imperviousness (Figure 8). Each criteria is assigned a weight from zero (least vulnerable) to one (most vulnerable). Application of weights to each criterion was conducted using the “Fuzzy Membership” tool of ArcGIS Spatial Analyst. Figure 9 showcases the applied weighting within the watershed for each criterion along with the sum of normalized criteria.

**Table 7. Vulnerability Criteria**

<b>Criteria</b>	<b>Description</b>	<b>Data Source</b>	<b>Weight</b>
Distance to Water body	Distance of area relative to a major water body such as a river. Higher weight assigned to small	Pinellas County	0 -1

	distances		
Slope	Higher weight assigned to relatively flat areas	From DEM (Pinellas County)	0 - 1
Elevation	Higher weight assigned to smaller elevations	DEM (Pinellas County)	0 - 1
Soil Condition	Higher weight applied to poorly drained soil (soil with higher runoff potential when wet).	USDA/NRCS Web Soil Survey	0-1
Imperviousness (%)	Runoff potential based upon level of imperviousness. Higher weight assigned to areas with low % imperviousness.	National Land Cover Database 2011	0-1



(a)

(b)

(c)

(d)

(e)

**Fig. 8: Non-weighted Vulnerability criterion (a) Distance, (b) Slope weight, (c) DEM, (d) Soil, and (e) Imperviousness for each vulnerability criteria for the Mariners Cove community. Source of Satellite Imagery: Esri, DigitalGlobe, GeoEye, Earthstar Geographics, CNES/Airbus DS, USDA, USGS, AeroGRID, IGN and GIS User Community.**

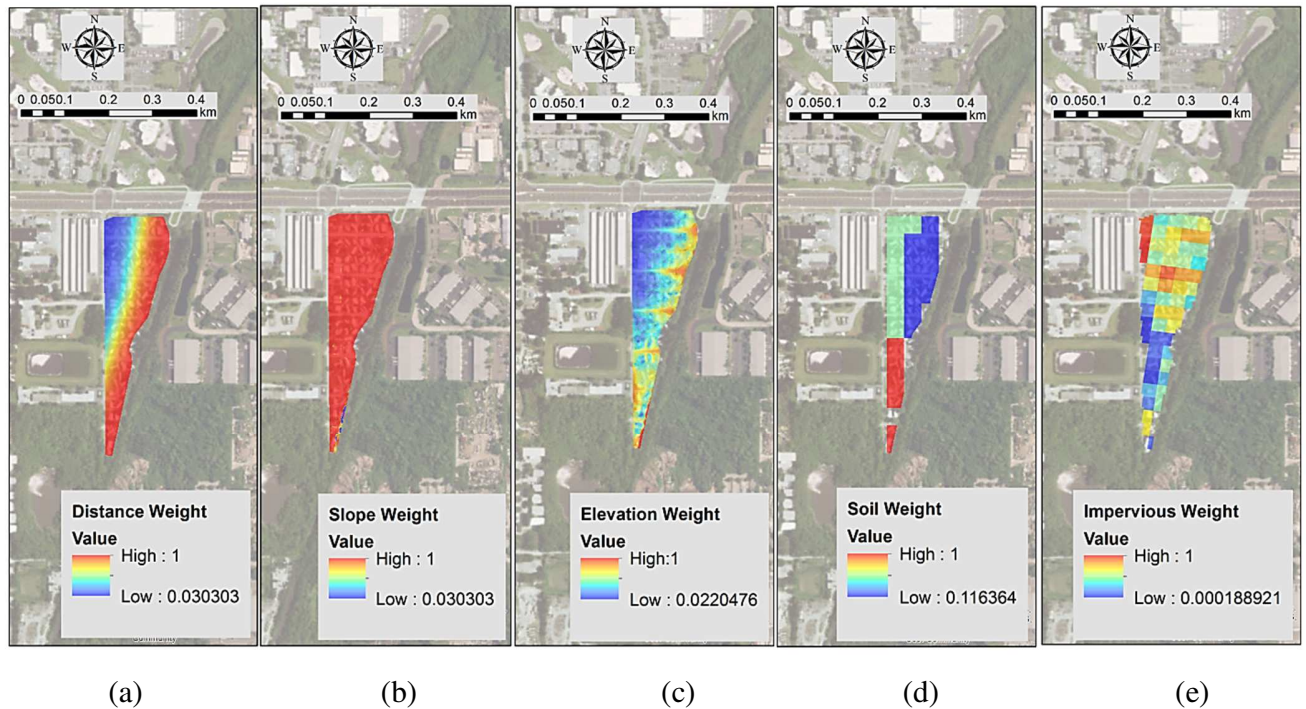


**Fig. 9: Associated weights (a) Distance, (b) Slope weight, (c) DEM, (d) Soil, and (e) Imperviousness for each vulnerability criteria for the Mariners Cove community. Source of Satellite Imagery: Esri, DigitalGlobe, GeoEye, Earthstar Geographics, CNES/Airbus DS, USDA, USGS, AeroGRID, IGN and GIS User Community.**

### **Exposure**

The exposure component of the risk formulation is an applied weight which is representative of the level of inundation due to the hazards considered. Tropical Storm Debby in late June 2012 was chosen as a test case for determining exposure due to its associated heavy rainfall, high tides, and waves. The level of inundation is determined via a watershed model, the Interconnected Channel and Pond Routing Version 4 software (ICPRv.4). The ICPRv.4 model

(Streamline Technologies Inc., 2015) is a comprehensive hydrodynamic stormwater and hydrologic model that integrates terrain data, hydrologic data, hydraulic data, and climate data via a layering and data management system. ICPRv.4 was utilized to construct a detailed model of the Cross Bayou watershed, which includes an integrated surface and groundwater interface. The ICPRv.4 software can also determine potential flood inundation via 2D overland flow algorithms. For more detail on ICPR software, please see Joyce et al. (2017).

***Adaptive Measures***

Four measures (Table 8) will be considered for defining adaptive capacity. Each measure will fall within three categories: blue, grey, and green, with their respective locations (Figure 10). From the three measures considered, each will be grouped under varying adaptive scenarios (Table 9).

**Table 8: Adaptive Measures**

<b>Measure</b>	<b>Description</b>	<b>Category of Drainage Infrastructure</b>
Canal Dredging(Section 1)	Removal of sediments and material from the Cross Bayou Canal to restore capacity of canal such as depth. Increase depth by 0.61m (2 ft.).	Blue
Canal Dredging(Section 2)	Removal of sediments and material from the Cross Bayou Canal to restore capacity of canal such as depth. Increase depth by 0.61m (2 ft.).	Blue
Tidal Wall (with stormwater inlets)	Protection against high tide events. Minimum height of wall = 3.04 m (10 ft.). Divert rainfall runoff using stormwater inlets with	Grey

	underground pipes back to canal downstream.	
Low Impact Development (LID)	Incorporation of natural drainage pathways to reduce runoff by reducing imperviousness by 25%	Green

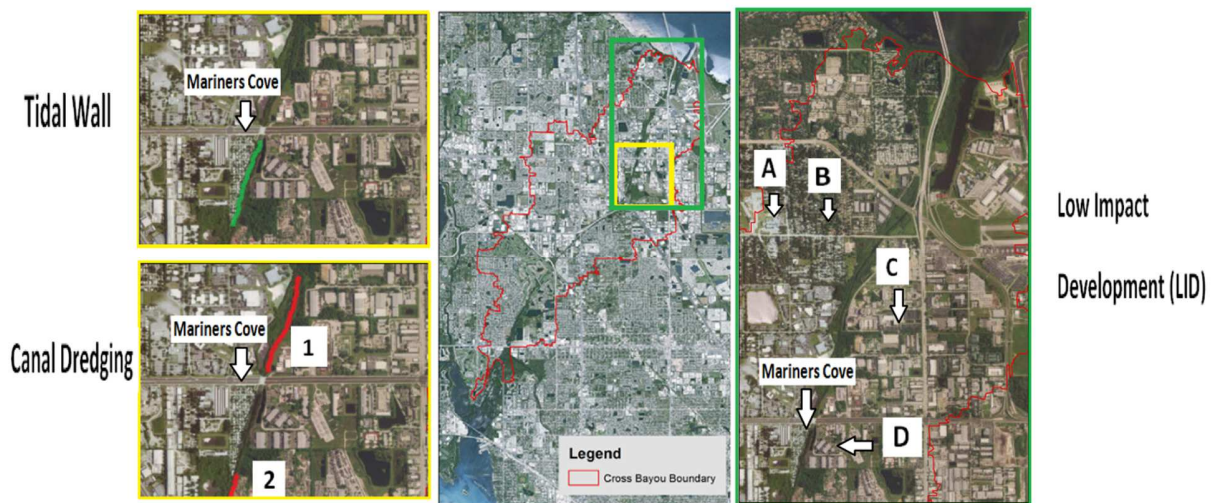


**Fig. 10: Locations of adaptive measures**

**Table 9: Adaptive Measures and Scenarios**

Scenario	Adaptive Measure(s)	Type and Location of Adaptive Measure(s)
1	No Action	None
2	LID Only	Site A (Pervious Pavement) Site B (Swales) Site C (Pervious Pavement) Site D (Pervious Pavement) (Figure 9)
3	Dredging Only	Sites 1 and 2 (Figure 9)
4	Tidal wall Only	Tidal Wall with stormwater



		inlets (Figure 9)
5	LID & Dredging	Site A (Pervious Pavement) Site B (Swales) Site C (Pervious Pavement) Site D (Pervious Pavement) (Figure 9) Sites 1 and 2 (Figure 9)
6	LID & Tidal wall	Site A (Pervious Pavement) Site B (Swales) Site C (Pervious Pavement) Site D (Pervious Pavement) Tidal Wall with stormwater inlets (Figure 9)
7	Dredging & Tidal wall	Tidal Wall with stormwater inlets Sites 1 and 2 (Figure 9)
8	LID, Dredging & Tidal wall	Site A (Pervious Pavement) Site B (Swales) Site C (Pervious Pavement) Site D (Pervious Pavement) (Figure 9) Sites 1 and 2 (Figure 9) Tidal Wall with stormwater inlets

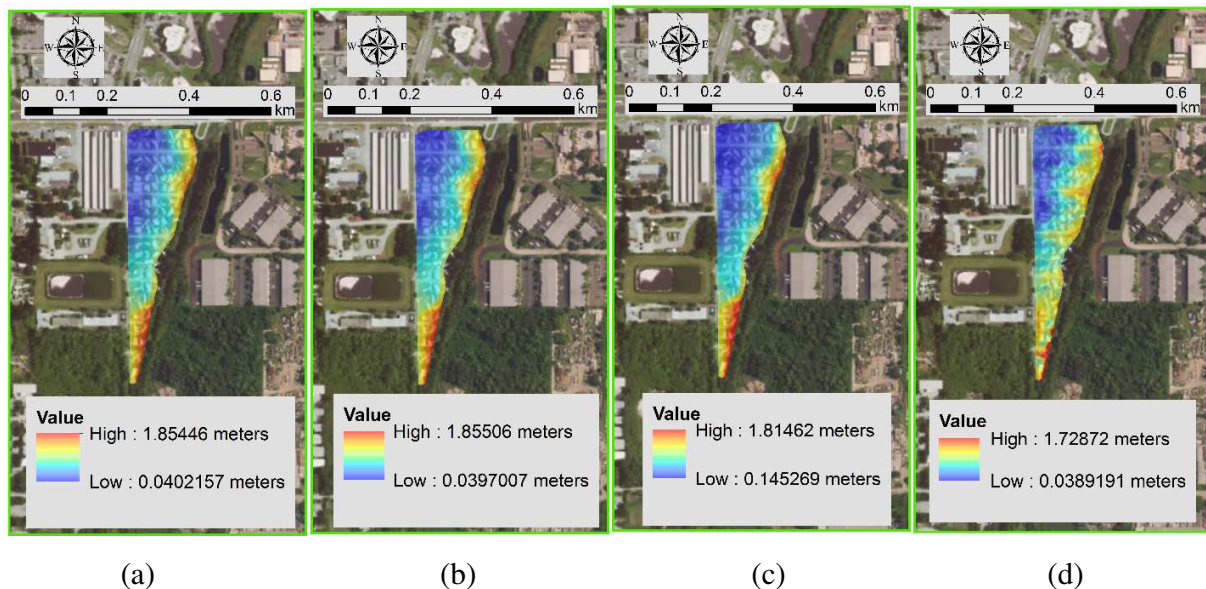
## RESULTS & DISCUSSION

### *Exposure*

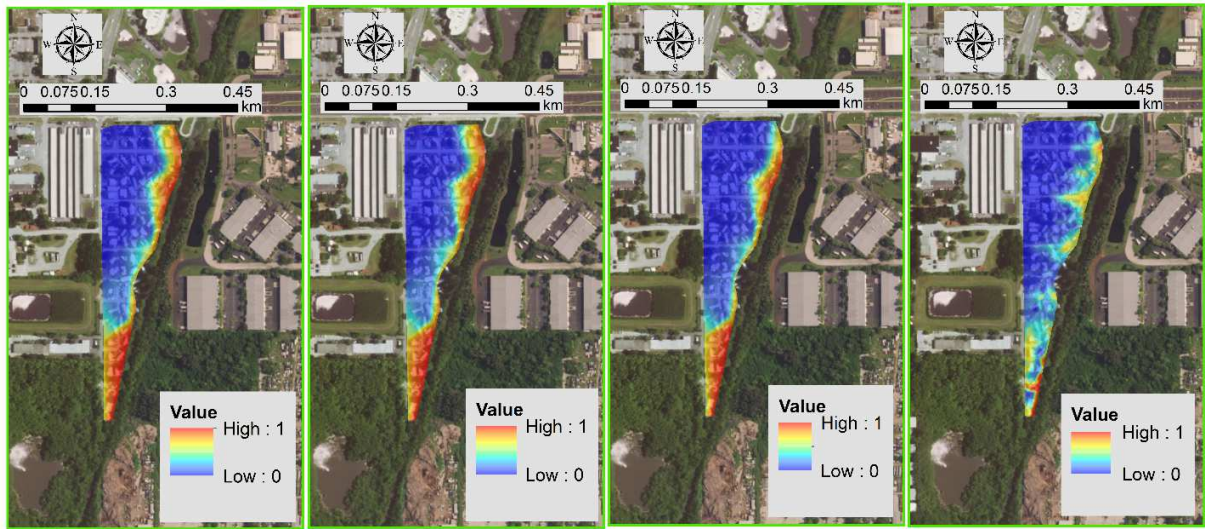
Exposure of the Mariners Cove community is presented in Figures 11 and 12 as a relation to inundation depth. Considering the scenarios presented in Table 9, the inundation depth is

higher with no adaptive measure as expected; however, incorporation of LID and dredging measures, without combined tidal wall and stormwater inlets, only offered minor reductions in inundation depths. This can be attributed to each adaptive measure offering a different level of resilience against disturbances such as flooding. Amongst the combination of adaptive measures, the incorporation of dredging and the tidal wall with stormwater inlets provides the greatest contribution to reducing the exposure magnitude or inundation depth (Figure 12c-d).

When considering spatial exposure changes, there are minor changes in exposure when incorporating adaptive measures without the tidal wall and stormwater inlets. With the incorporation of the tidal wall and stormwater inlets, changes in spatial exposure are more pronounced with an unexpected result such that areas near the tidal wall and stormwater inlets are slightly more exposed spatially; however, exposure magnitudes are still considerably lower compared to scenarios when no adaptive action was considered. Exposure only explains one aspect of risk that can be explained further when considering resilience, since the incorporation of resilience can essentially determine how long the exposure is felt within the area of concern. For instance, for what time period will the area of concern be exposed or inundated and in what time period will the flood water begin to recede? Answers to these questions can be provided by the results of the resilience metric.

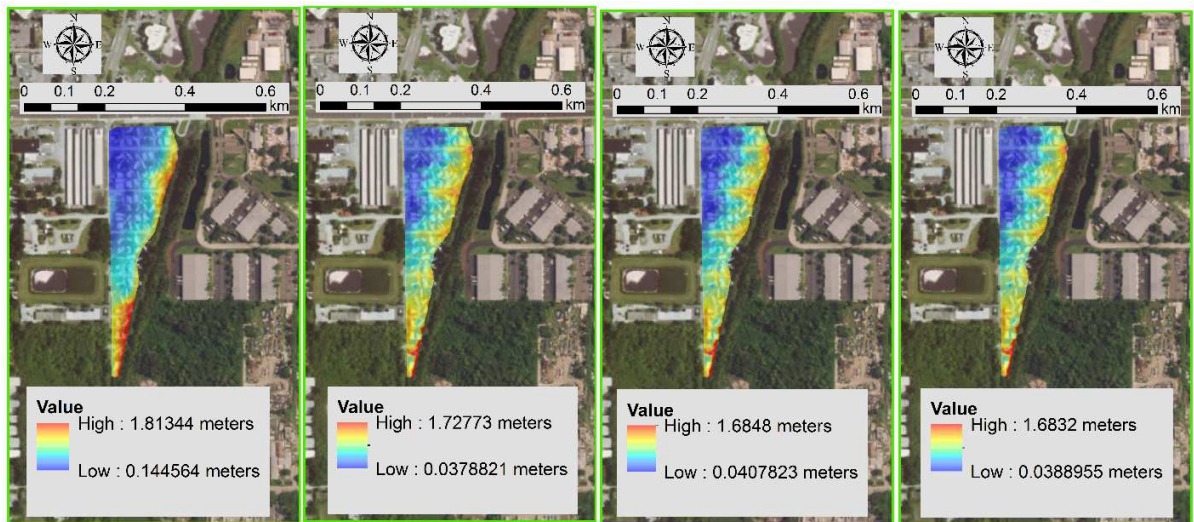






(e) (f) (g) (h)

**Fig. 11: Non-normalized exposure (flood depth) for (a) no adaptive action, (b) LID Only, (c) Dredging Only and (d) Wall Only as well as normalized exposure for (e) no adaptive action, (f) LID Only, (g) Dredging Only and (h) Wall Only during Tropical Storm Debby on June 24<sup>th</sup>, 2012 Hour 18 (during max exposure).**



(a) (b) (c) (d)

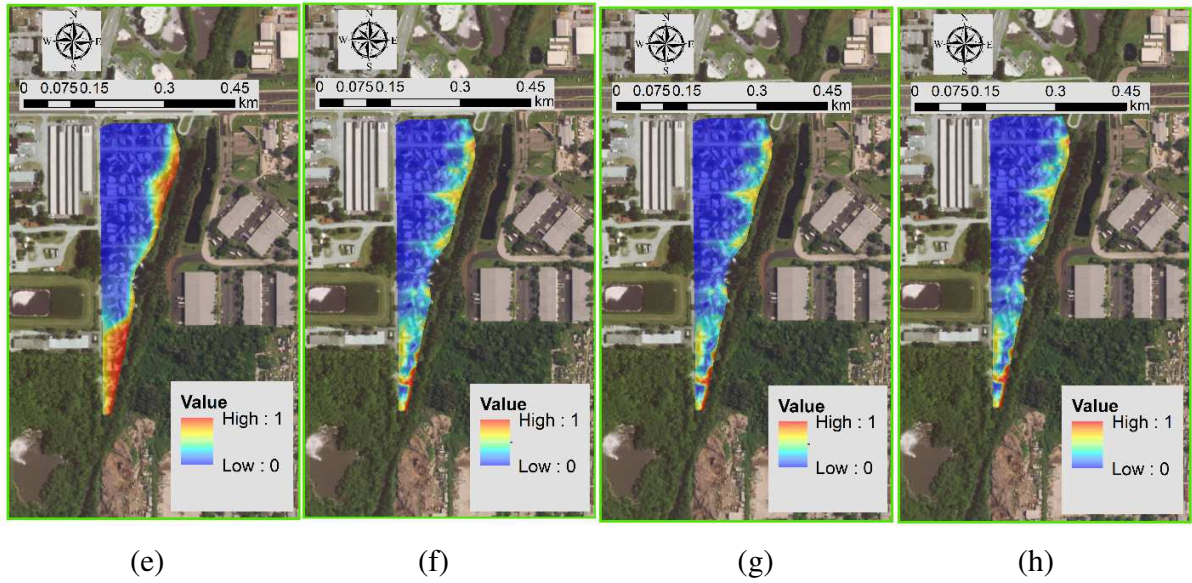


**Fig.12: Non-normalized exposure (flood depth) for (a) LID & Dredging, (b) LID & Wall, (c) Dredging & Wall and (d) LID, Dredging & Wall as well as normalized exposure for (e) LID & Dredging, (f) LID & Wall, (g) Dredging & Wall and (h) LID, Dredging & Wall during Tropical Storm Debby on June 24<sup>th</sup>, 2012 Hour 18(during max exposure).**

### ***Resilience***

The goal of the resilience metric is to minimize the difference between the initial recovery time  $T_i$  and the final recovery time [i.e., the numerator ( $T_f - T_i$ ) such that the system in question can achieve recovery in a shorter period of time such that  $T_f - T_i$  is small in value]. As evident in Table 10, the combination of dredging and the tidal wall resulted in minimizing the difference between the initial recovery time  $T_i$  and the final recovery time [i.e., the numerator ( $T_f - T_i$ )] such that this combination resulted in faster overall recovery or greater resilience to flood waters.

**Table 10: Recovery Time and Resilience Term**

Scenario	ICPRv.4 Simulation Results		Relative Change in Time of Exposure $\frac{T_f - T_i}{T_i}$	Resilience $\frac{1}{\left[ \frac{T_f - T_i}{T_i} \right]}$
	Initial Recovery Period Post-Max Flooding $T_i$ (hours)	Final (Full) Recovery Period Post-Max Flooding $T_f$ (hours)		
No Action	14	120	7.57	0.132
LID Only	14	120	7.57	0.132
Dredging Only	13	99	6.61	0.151
Wall Only	13	28	1.15	0.870
LID & Dredging	13	99	6.61	0.151
LID & Wall	13	28	1.15	0.870
Dredging & Wall	12	25	1.08	0.926
LID, Dredging & Wall	12	25	1.08	0.926

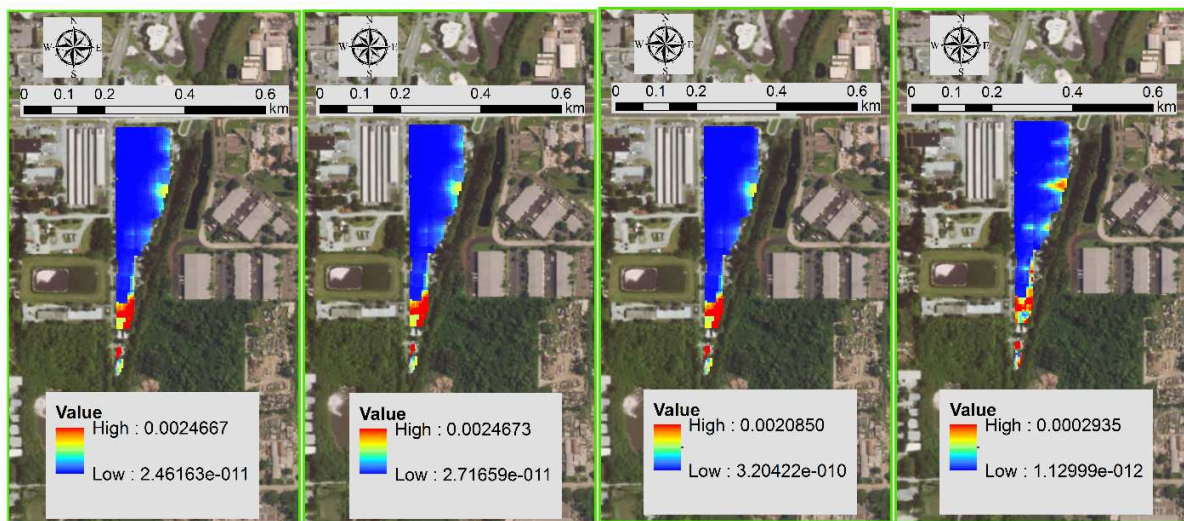
***Risk***

Given the eight scenarios considered, the hazard and vulnerability components were the same. The primary components that influenced changes in risk were exposure and resilience, which are tied to the adaptive measures implemented. According to Eq. 12, the expected value of risk change decreases considerably for adaptive measures incorporating the tidal wall (Figure 13). Reduction in risk magnitudes overall (Figure 13a-h) with the incorporation of adaptive



measures such as LID, dredging and the tidal wall, can be attributed to an increase in flood resilience. Irrespective of changes to exposure magnitudes, resilience remains the greatest influence to risk such that increases in flood resilience (i.e., decreases in the time for water to recede from the area) via incorporation of adaptive measures presented in Table 10, help to offset risk magnitudes as evident in Figure 13.

Spatially, risk does not change much across adaptive measures, with the exception of the southwestern corner of the Mariners Cove area and the eastern boundary of the Mariners Cove area (Figure 14). The changes in risk, spatially, near the southwestern corner and eastern boundary of Mariners Cove are attributable to incorporation of the tidal wall and stormwater inlets. In general, the closer to the southern Mariners Cove boundary, the higher the risk. Overall, each adaptive measure offers a different level of resilience against flood disturbances and subsequently offers differing changes in risk, more so by magnitude than spatially.

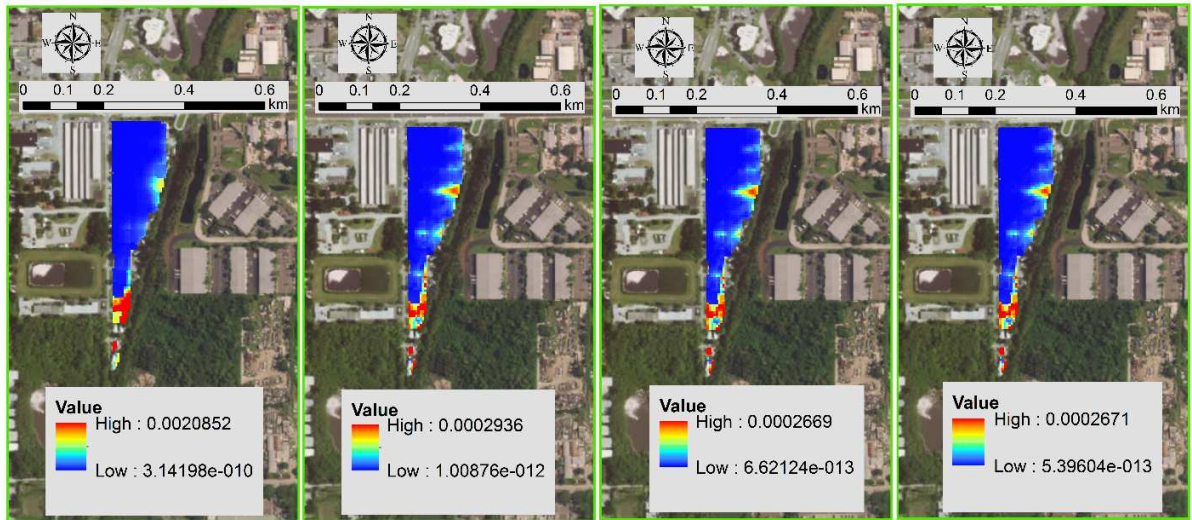


(a)

(b)

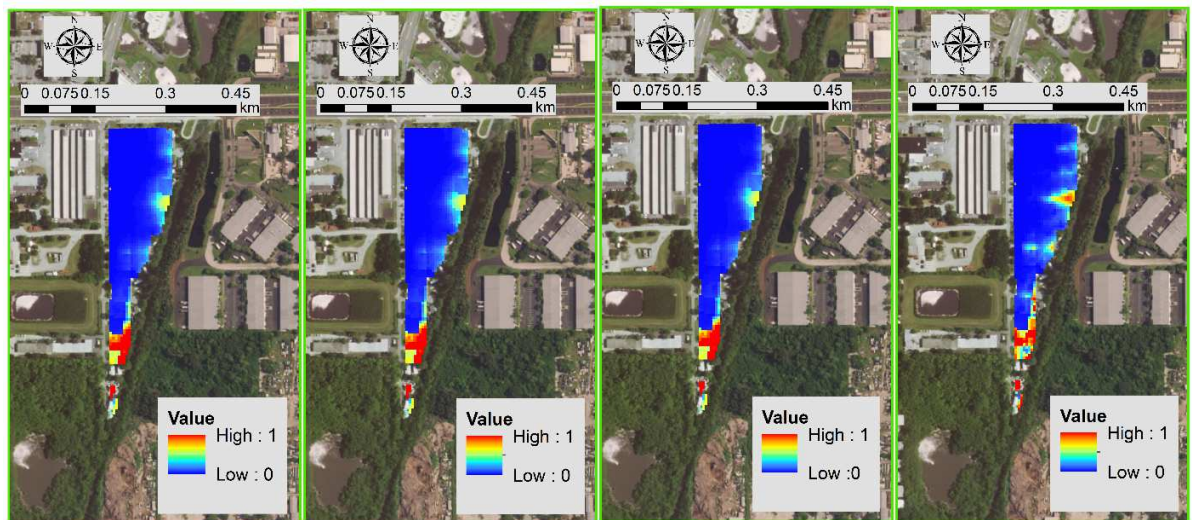
(c)

(d)



(e) (f) (g) (h)

**Fig. 13: Non-normalized spatial risk values for (a) no adaptive action, (b) LID Only, (c) Dredging Only and (d) Wall Only during Tropical Storm Debby on June 24<sup>th</sup>, 2012 Hour 18 (during max exposure). Non-normalized spatial risk values for (e) LID & Dredging, (f) LID & Wall, (g) Dredging Only and (h) Wall Only during Tropical Storm Debby on June 24<sup>th</sup>, 2012 Hour 18 (during max exposure).**



(a) (b) (c) (d)



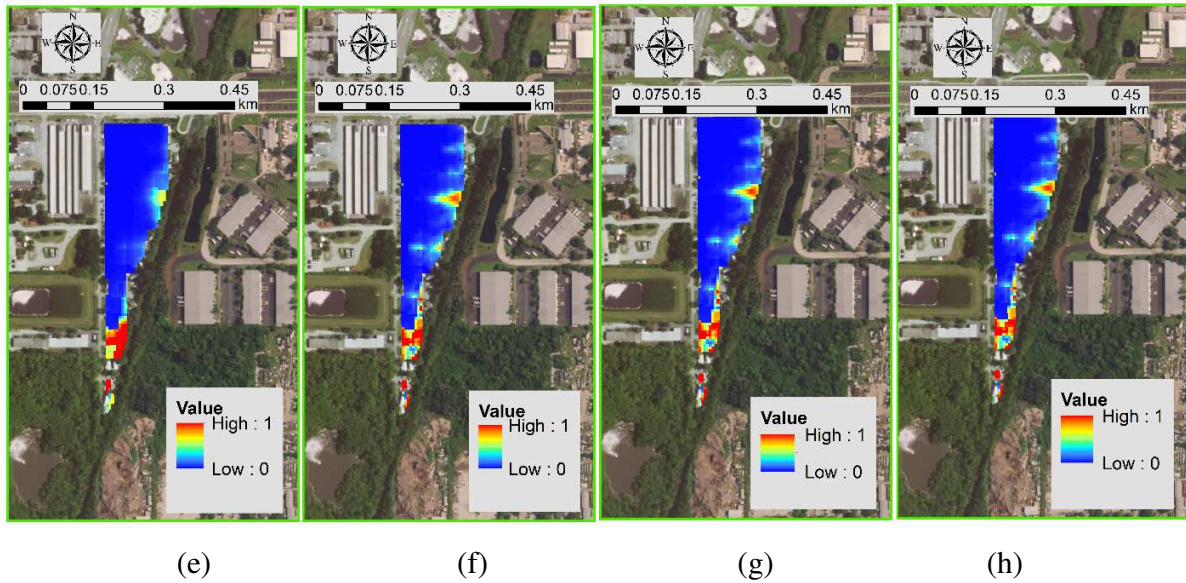


**Fig. 14: Normalized spatial risk for (a) no adaptive action, (b) LID Only, (c) Dredging Only and (d) Wall Only during Tropical Storm Debby on June 24<sup>th</sup>, 2012 Hour 18 (during max exposure). Normalized spatial risk for (e) LID & Dredging, (f) LID & Wall, (g) Dredging and Wall and (h) LID, Dredging and Wall during Tropical Storm Debby on June 24<sup>th</sup>, 2012 Hour 18 (during max exposure).**

When conducting risk analysis for future hazards, there are sources of uncertainty which could be aleatory or epistemic in nature (Der Kiureghian and Ditlevsen, 2009) such that uncertainty arises from the process itself or intrinsic uncertainty (aleatory) and uncertainty from lack of knowledge or data in modelling the process (epistemic).

### ***Decision Analysis***

Decision makers often rely on criteria and weighing possible outcomes before choosing the most beneficial plan of action. This particularly concerns municipalities evaluating potential measures for improving infrastructure for their constituents to rely on. This is particularly evident in areas that are prone to flooding and often rely on adequate drainage infrastructure to minimize damage to property. This is important from the vantage point of national policies related to flood risk and insurance. The National Flood Insurance Program (NFIP) aims to reduce the impact of flooding on private and public property by providing affordable insurance to property owners. The Community Rating System (CRS) of the NFIP is a voluntary program that encourages communities to adopt and enforce flood management practices which exceed NFIP

requirements as an incentive for reducing flood insurance premiums. Recommended flood management practices under CRS include flood protection measures such as structural projects along with drainage system maintenance and improving flood risk mapping. The adaptive measures considered in the study such as LID, the tidal wall with stormwater inlets, and dredging are examples of such recommended flood management practices.

With respect to decision analyses, weighting criteria can be a useful approach toward choosing a beneficial plan of action. Both tables (Table 11 and Table 12) showcase the non-weighted criteria values and weighted criteria values for 5 criteria including: initial recovery time, final recovery time, capital investment effort, areal-average risk, and areal-average exposure. The initial and final recovery times have been previously defined as related to the resilience metric. The capital investment effort is the capital investment required to implement the proposed adaptive measure and is assigned a value from 0 to 3, with 0 indicating no capital investment and 3 indicating large capital investment. The areal-average risk and areal-average exposure are the areal means of the risk value and exposure or inundation depth, respectively, over the entire area of concern. Figure 15 provides a visual representation of Table 12 for decision makers.

**Table 11. Non-Weighted Decision Criteria**

Scenario	Decision Criterion				
	Initial Recovery Time (hrs)	Final Recovery Time (hrs)	Capital Investment Effort	Areal-Average Risk Value	Areal-Average Exposure (meters)
No Action	14	120	0	0.05	0.697
LID Only	14	120	1	0.05	0.697
Dredging Only	13	99	2	0.0456	0.662
Wall Only	13	28	2	0.0369	0.528

LID & Dredging	13	99	3	0.0456	0.661
LID & Wall	13	28	3	0.0369	0.527
Dredging & Wall	12	25	3	0.0342	0.483
LID, Dredging & Wall	12	25	3	0.0341	0.481

**Table 10. Weighted Decision Criteria**

Scenario	Decision Criterion				
	Initial Recovery Time	Final Recovery Time	Capital Investment Effort	Areal-Average Risk Value	Areal-Average Exposure
No Action	1.000	1.000	0.000	1.000	1.000
LID Only	1.000	1.000	0.333	1.000	1.000
Dredging Only	0.929	0.825	0.667	0.912	0.950
Wall Only	0.929	0.233	0.667	0.738	0.758
LID & Dredging	0.929	0.825	1.000	0.912	0.948
LID & Wall	0.929	0.233	1.000	0.738	0.756
Dredging & Wall	0.857	0.208	1.000	0.684	0.693



LID, Dredging & Wall	0.857	0.208	1.000	0.682	0.690
----------------------------	-------	-------	-------	-------	-------

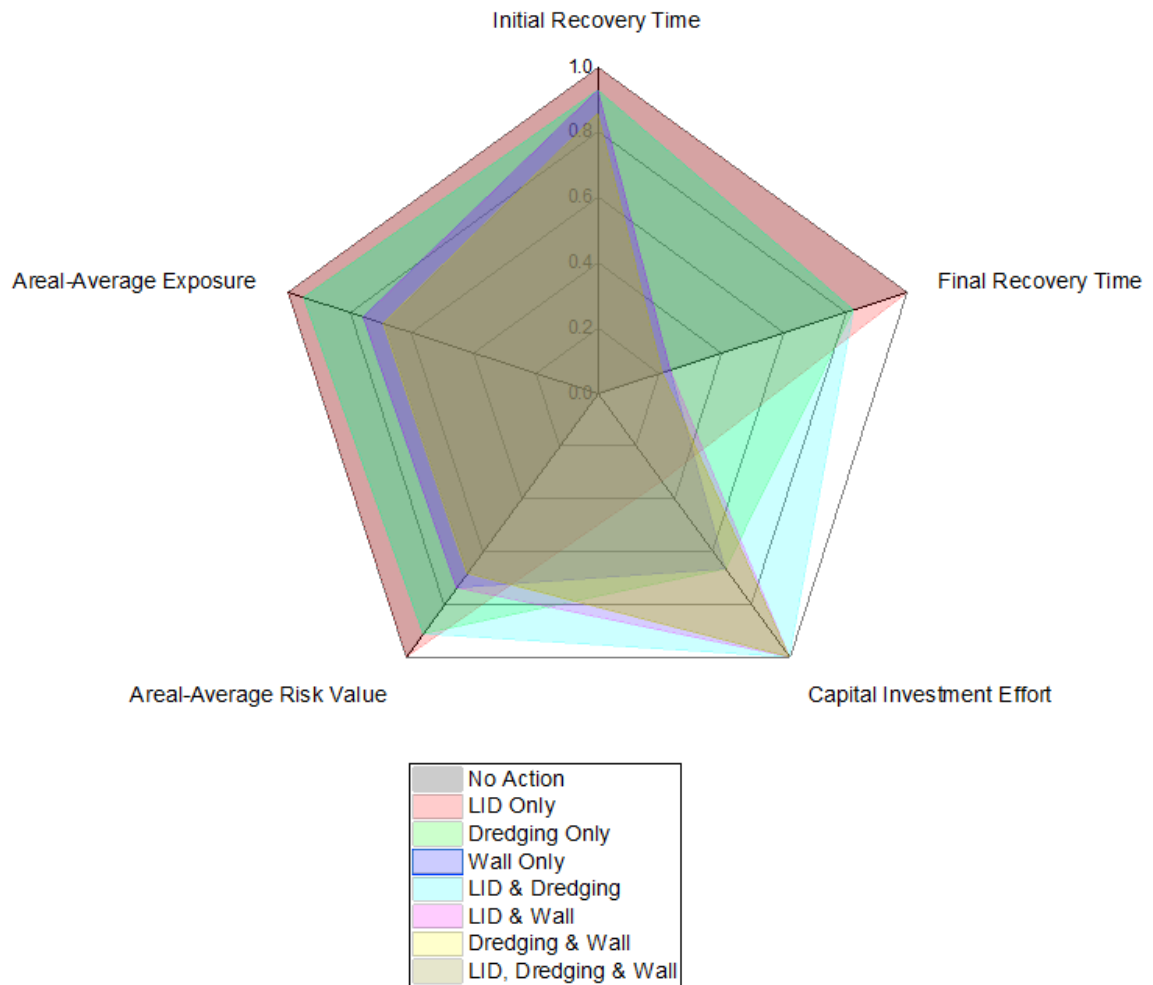


**Fig. 15: Radar plot of weighted criteria for no action and 7 adaptive measures**

As evidenced by the information in Table 12 and Figure 15, either the alternative with dredging and the tidal wall or the alternative with LID, dredging and the tidal wall should be chosen as the most beneficial plan of action for decision makers. Both adaptive measures provide the lowest areal-average risk, the lowest areal-average exposure and minimal initial and final recovery time, although capital investment costs would be higher.

## CONCLUSION

Assessing flood risk for decision making requires identifying components of risk and quantifying these components by an integrative approach. Components associated with risk include hazard, vulnerability, exposure, and resilience in the form of adaptive capacity. Vulnerability, exposure, and resilience are dependent on the hazard(s) considered, while vulnerability is dependent on adaptive capacity, which is tied to resilience. Hence, risk can vary primarily due to hazard(s) considered and the associated level of resilience for such hazard(s). Specifically, for infrastructure, resilience is tied to the level of recovery given the hazard(s) considered, which could be interdependent. This has implications for decision makers such as municipalities, who may rely on risk being fixed and do not consider interdependent hazards, adaptive measures, and resilience (as a function of adaptive measures and hazards). As such this study addresses approaches in considering resilience in overall flood risk management analysis and determines if coupling flood risk and engineering resilience, via adaptive measures, could improve flood impact assessment. As a result, this study notes this approach has implications for decisions makers such as municipalities and their constituents on a policy level when considering existing flood insurance mapping methodologies.

Incorporating resilience within risk framework, as it pertains to drainage infrastructure systems, is inherently important for such systems to reduce flood risk. Particularly for engineered drainage infrastructure systems with adaptive capacity such as LID and flood proofing structure, risk is typically considered for a low probable, damaging event for design purposes. In this study, risk is no longer fixed for an entire area but varies spatially, which could vary with hazards considered and adaptive measures adopted. With this advancement, resilience becomes an important factor for determining the performance of drainage infrastructure and flood protection during a major flood event. The resilience term was determined from observing time of water receding (i.e., time of recovery via the system). The time between the initial and final (full) water receding from an area of concern is a useful parameter for determining resilience of drainage infrastructure systems toward flooding. The shorter the time period for water to fully recede during flooding, the more resilient the system and vice-versa. This study indicates that either the alternative with dredging and the tidal wall or the alternative with LID, dredging, and

the tidal wall should be chosen as the most beneficial plan of action for the community considered. Enacting a system for which flood waters can recede within a shorter time frame can reduce exposure and subsequently reduce damage and overall risk to flooding. Our case study has fully confirmed this suite of new concepts within the context of a coupled risk and resilience framework. Future work may be extended to tackle different types of flooding events for inland cities as well.

Nevertheless, key limitations of this study include the relation of vulnerability to resilience within the risk formulation. For the purposes of this study, the vulnerability metric does not change with space and time, however implementation of adaptive measures (see Table 8) represents a link between vulnerability and resilience. Allowing changes to the vulnerability metric in space and time, dynamically, was not a motivation of this study and was instead accounted for by incorporation of the adaptive measures, which can be used to offset existing vulnerability and provide a path toward resilience.

#### **ACKNOWLEDGEMENTS**

The authors are grateful for the financial support of the Florida Sea Grant College Program, a partnership between the Florida Board of Education, the National Oceanic and Atmospheric Administration, and Florida's citizens and governments, under project R-CS-58 with assistance from the Pinellas County Government and to Southwest Florida Water Management District for making rainfall data available. The authors are thankful for the constructive and copious comments received from anonymous reviewers who helped improve the quality of the paper.

## APPENDIX

### Appendix A: Curve Fitting & Goodness of Fit Test

**Table A.1: Marginal Distribution for Each Variable (For Target Year 2012)**

Variable	Fitted Distribution	Parameter(s) [location, scale, shape]
Tidal Stage	Generalized Extreme Value	[0.1836,0.1209,0.4494]
Rainfall	Generalized Extreme Value	[2.766,6.261e-04,2.190e-04]
Wind Speed	Generalized Extreme Value	[-0.1232,2.204,6.932]
Wave Height	Generalized Extreme Value	[0.2545,0.1488,0.2576]

**Table A.2: Goodness of Fit Tests (For Target Year 2012)**

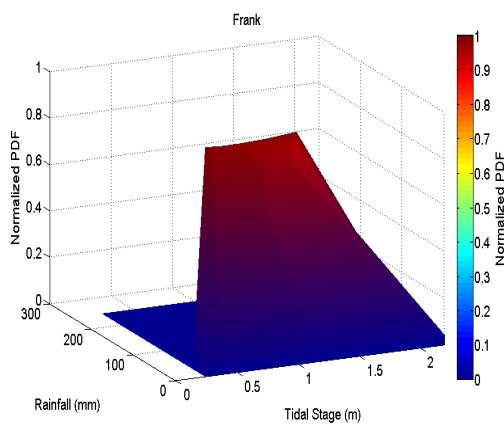
Variable	# of Data points	Null Hypothesis	p-value	Chi-Squared	K-S
Tidal Stage	366	Data are consistent with proposed statistical distribution in Table 7	0.05	Rejects null hypothesis	Does not reject null hypothesis at 5% significance level
Rainfall	366	Data are consistent with proposed statistical distribution in Table 7	0.05	Does not reject null hypothesis at 5% significance level	Rejects null hypothesis
Wind Speed	366	Data are	0.05	Rejects null	Rejects null

		consistent with proposed statistical distribution in Table 7		hypothesis	hypothesis
Wave Height	366	Data are consistent with proposed statistical distribution in Table 7	0.05	Rejects null hypothesis	Does not reject null hypothesis at 5% significance level

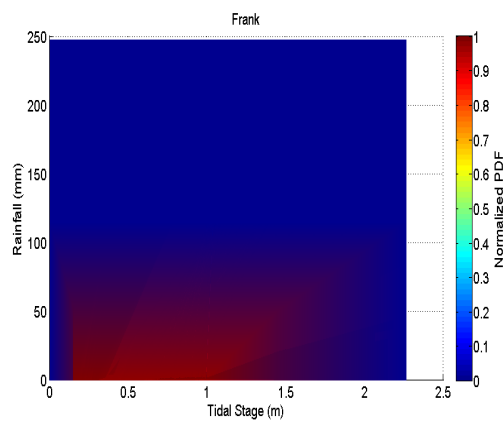
**Appendix B: Copula Analysis (For Target Year 2012)**

**Table B.1: Copula Analysis for Hazard Variables**

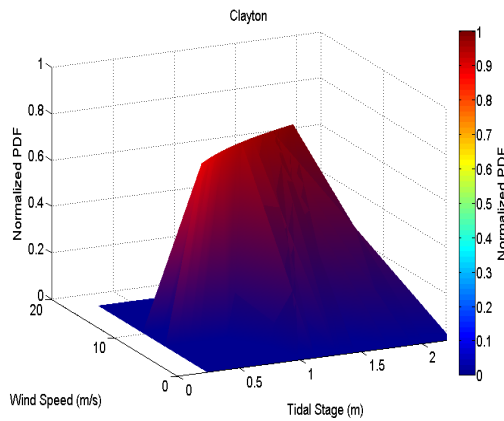
Copula Family	<i>Tidal Stage vs. Rainfall</i>			<i>Tidal Stage vs. Wind Speed</i>			<i>Tidal Stage vs. Wave Height</i>		
	Max. Log Likelihood Value	Dependence Parameter ( $\theta$ )	AIC	Max. Log Likelihood Value	Dependence Parameter ( $\theta$ )	AIC	Max. Log Likelihood Value	Dependence Parameter ( $\theta$ )	AIC
<i>Gumbel</i>	8.55e-14	1.00	72.2	-1.405e-14	1.00	75.8-6.28i	-4.47e-15	1.00	78.1 - 6.28i
<i>Clayton</i>	577.7	0.100	-0.7182	-67.06	0.100	3.59-6.28i	9.67e+02 - 1.093e+01i	0.675	-1.748 + 0.0226i
<i>Frank</i>	-1.417e+05	0.100	-11.7 +6.26i	-42.22	0.100	4.51-6.28i	142.7	0.100	2.08



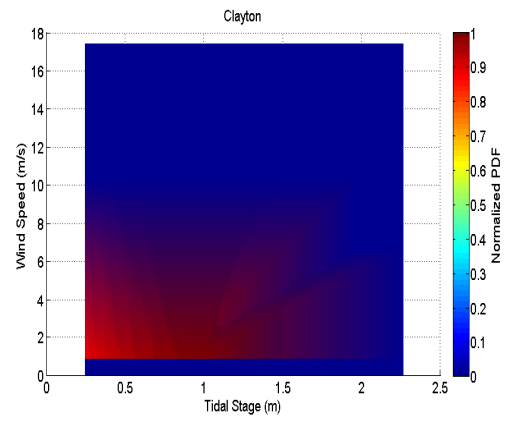
**(a)**



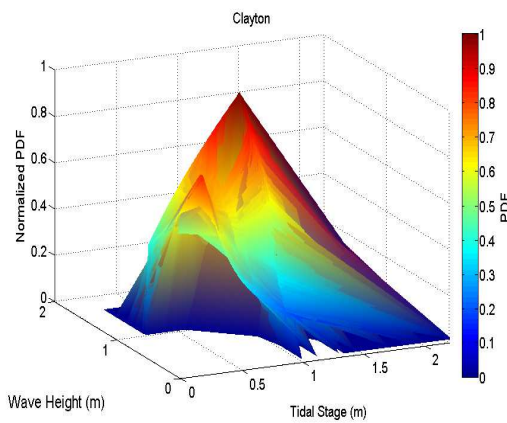
**(b)**



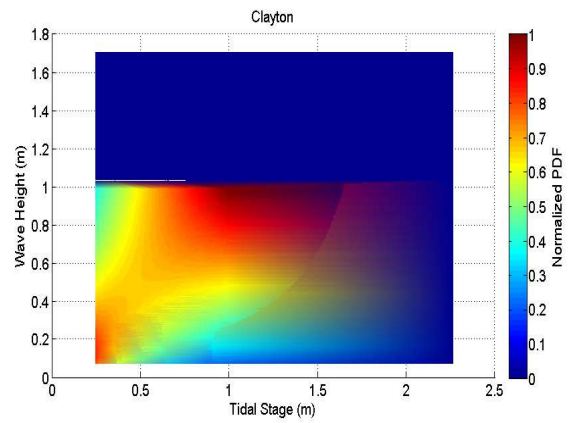
(c)



(d)



(e)



(f)

**Fig.B.1: (a) Frank PDF plot of Rainfall and Tidal Stage (3D view) with (b) Rainfall and Tidal Stage (top view) for target year 2012 (c) Clayton Wind Speed and Tidal Stage (3D view) with (d) Wind Speed and Tidal Stage (top view) for target year 2012 and (e) Clayton PDF plot of Wave Height and Tidal Stage (3D view) with (f) Wave Height and Tidal Stage (top view) for target year 2012.**

## REFERENCES

Akaike H. 1974. A new look at the statistical model identification. *IEEE Trans. Autom. Control*, 19:716–722.

Ali, M.M., Mikhail, N.N., Haq, M.S., 1978: A class of bivariate distributions including the bivariate logistic. *J. Multivar. Anal.*, 8 (3):405–412.

Bahadur, A. V., Ibrahim, M., and Tanner, T., 2010: The resilience renaissance? Unpacking of resilience for tackling climate change and disasters. Institute of Development Studies (for the Strengthening Climate Resilience (SCR) consortium): Brighton, UK

Balistracchi, M. and Bacchi, B., 2011: Modelling the statistical dependence of rainfall event variables by a trivariate copula function. *Hydrol. Earth Syst. Sci.*, 15:1959–1977. doi:10.5194/hess-15-1959-2011

Chebana F, Ouarda TBMJ., 2011: Multivariate quantiles in hydrological frequency analysis. *Environmetrics*, 22:63-78. Cleophas,T.J. and Zwinderman, A.H., 2013: Bayesian Networks.*Machine Learning in Medicine*. [https://doi.org/10.1007/978-94-007-6886-4\\_16](https://doi.org/10.1007/978-94-007-6886-4_16)

Ciurean, R. L., Schroter, D., & Glade, T. (2013). Conceptual Frameworks of Vulnerability Assessments for Natural Disasters Reduction. In J. Tiefenbacher, Approaches to Disaster Management - Examining the Implications of Hazards, Emergencies and Disasters. Retrieved from <http://www.intechopen.com/books/approaches-to-disaster-management-examining-the-implications-of-hazards-emergencies-and-disasters/conceptualframeworks-of-vulnerability-assessments-for-natural-disasters-reductio>

Clayton, D.G., 1978: A model for association in bivariate life tables and its application in epidemiological studies of familial tendency in chronic disease incidence. *Biometrika*, 65 (1): 141–151.

Corbella, S. and Stretch, D.D., 2013: Simulating a multivariate sea storm using Archimedean copulas. *Coastal Engineering* 76: 68-78.

De Bruijn, K.M., 2005: Resilience and flood risk management. A systems approach applied to lowland rivers. PhD thesis. Delft University of Technology, Delft, The Netherlands.

De Michele, C. and Salvadori, G., 2003: A generalized Pareto intensity-duration model of storm rainfall exploiting 2-copulas. *J. Geophys. Res., [Atmos.]*, 108(D2), ACL 15-1–ACL 15-11.

- De Michele, C., Salvadori, G., Canossi, M., Petaccia, A., Rosso, R., 2005: Bivariate statistical approach to check adequacy of dam spillway. *J. Hydrol. Eng.*, 10 (1): 50–57.
- De Michele, C., Salvadori, Passoni, G., Vezzoli, R., 2007: A multivariate model of sea storms using copulas. *Coastal Engineering* 54: 734-751
- Der Kiureghian, A., and Ditlevsen, O., 2009: Aleatory or epistemic? Does it matter?, *Structural Safety*, 31(2): 105-112, ISSN 0167-4730, <http://dx.doi.org/10.1016/j.strusafe.2008.06.020>.
- Favre, A.C., El Adlouni, S., Perreault, L., Thiémondge, N., Bobée, B., 2004: Multivariate hydrological frequency analysis using copulas. *Water Resour. Res.*, 40 (1): W01101.
- Food and Agriculture Organization, 2003: The Role of Local Institutions in Reducing Vulnerability to Recurrent Natural Disasters and in Sustainable Livelihoods Development in High Risk Areas. Produced by Economic and Social Development Department. Available online at [<http://www.fao.org/wairdocs/ad695e/ad695e01.htm>].
- Francis, R., & Bekera, B. (2014). A metric and frameworks for resilience analysis of engineered and infrastructure systems. *Reliability Engineering and System Safety*, 121: 90 - 103.
- Frank, M.J., 1979: On the simultaneous associativity of  $F(x, y)$  and  $x + y - F(x, y)$ . *Aequationes Math.*, 19 (1): 194–226.
- Gumbel, E.J., 1960: Distributions des valeurs extrêmes en plusieurs dimensions. *Publ. Inst.Stat. Univ. Paris*, 9: 171–173.
- Holling, C.S., 1973: Resilience and stability of ecological systems. *Annual Review of Ecology and Systematics*, 1–23
- IPCC, 2014: Summary for Policymakers. In: Climate Change 2014: Impacts, Adaptation, and Vulnerability. Part A: Global and Sectoral Aspects. Contribution of Working Group II to the Fifth Assessment Report of the Intergovernmental Panel on Climate Change [Field, C.B., V.R. Barros, D.J. Dokken, K.J. Mach, M.D. Mastrandrea, T.E. Bilir, M. Chatterjee, K.L. Ebi, Y.O. Estrada, R.C. Genova, B. Girma, E.S. Kissel, A.N. Levy, S. MacCracken, P.R. Mastrandrea, and L.L.



White (eds.)). Cambridge University Press, Cambridge, United Kingdom and New York, NY, USA, pp. 1-32.

Joe, H., 1993: Parametric families of multivariate distributions with given margins. *J. Multivar. Anal.* 46 (2): 262–282.

Joe, H., 1997: Multivariate models and dependence concepts. *Monographs on Statistics and Applied Probability Vol. 73*. Chapman & Hall, London, UK.

Johansen, I. L., 2010: Foundations of Risk Assessment. Norwegian University of Science and Technology (NTNU).

Jones Edmunds and Associates, Inc., 2013: Floodplain Analysis, Cross Bayou Watershed Management Plan. Pinellas County Board of County Commissioners and Southwest Florida Water Management District.

Jordanger, L. A. and Tjostheim, D., 2014: Model selection of copulas: AIC versus a cross validation copula information criterion. *Statistics and Probability Letters*, 92(1): 249-255.

Joyce, J., Chang, N. B., Harji, R., Ruppert, T., and Imen, S., 2017: Developing a multi-scale modeling system for resilience assessment of green-grey drainage infrastructures under climate change and sea level rise impact. *Environmental Modelling and Software*, 90: 1-26.

Khadka, M. S., 2008: Parameter estimation of Copula using maximum likelihood estimation (MLE) method. Oklahoma State University, ProQuest Dissertations Publishing.

Klein R.J.T, Nicholls R.J., and Thomalla F.T., 2003: Resilience to natural hazards: how useful is this concept? *Environ Hazards* 5:35–45. doi:10.1016/j.hazards.2004.02.001

Luers, A.L., Lobell, D.B., Sklar, L.S., Addams, C.L, Matson, P.A., 2003: A method for quantifying vulnerability, applied to the agricultural system of the Yaqui Valley, Mexico. *Global Environmental Change* 13:255-267.

Nelsen, R.B., 2006. An Introduction to Copulas, Springer Series in Statistics. Springer, NewYork, USA.

NOAA, 2016: Sea Level Trends. Accessed August 2016. [Available online at <https://tidesandcurrents.noaa.gov/sltrends/sltrends.html>]

Omer, M., 2013: The resilience of networked infrastructure systems. World Scientific.

Park, J., Seager, T. P., Rao, P. S. C., Convertino, M. and Linkov, I., 2013: Integrating Risk and Resilience Approaches to Catastrophe Management in Engineering Systems. *Risk Analysis*, 33: 356–367. doi:10.1111/j.1539-6924.2012.01885.x

Patton, A., 2004: On the Out-of-Sample Importance of Skewness and Asymmetric Dependence for Asset Allocation, *Journal of Financial Econometrics*, 2(1): 130-168

Salvadori, G and De Michele, C., 2004: Frequency analysis via copulas: theoretical aspects and applications to hydrological events. *Water Resour Res*, 40:W12511. doi:10.1029/2004WR003133

Streamline Technologies, Inc., 2015: An Integrated Surface Water-Groundwater Model of the Cross Bayou Watershed

Trepanier, J.C., Needham, H.F., Elsner, J.B., and Jagger, T.H., 2014: Combining Surge and Wind Risk from Hurricanes Using a Copula Model: An Example from Galveston, Texas, *The Professional Geographer*, DOI:10.1080/00330124.2013.866437

Wahl, T., Muddersbach, C., Jensen, J., 2012: Assessing the hydrodynamic boundary conditions for risk analyses in coastal areas: a multivariate statistical approach based on Copula functions. *National Hazards and Earth Syst. Science*, 12, 495–510

Wahl, T., Jain, S., Bender, J., Meyers, S.D. and Mark E. Luther 2015:Increasing risk of compound flooding from storm surge and rainfall for major US cities, *Nature Climate Change*, doi:10.1038/nclimate2736

Wang, C., Chang, N.-B., and Yeh, G. (2009). Copula-based flood frequency (COFF) analysis at the confluences of river systems. *Hydrological Process*, 23:1471–1486.

World Health Organization, 2007: Risk reduction and emergency preparedness: WHO six-year strategy for the health sector and community capacity development. WHO Document Production Services, Geneva, Switzerland.

UNISDR (United Nations International Strategy for Disaster Reduction), 2002: SDR background paper for WSSD. Geneva: UN

Uusitalo, L., 2007: Advantages and challenges of Bayesian networks in environmental modelling, *Ecological Modelling*, 203 (3–4): 312-318, <https://doi.org/10.1016/j.ecolmodel.2006.11.033>.

Xu, K., Ma, C., Lian, J. and Bin, L., 2014: Joint probability analysis of extreme precipitation and storm tide in a coastal city under changing environment. *PLoS One*, 9(10): e109341. doi: 10.1371/journal.pone.0109341.

Yodo, N. and Wang, P., 2016: Engineering Resilience Quantification and System Design Implications: A Literature Survey, *Journal of Mechanical Design*, 138(11): 111408 (13 pages) Paper No: MD-16-1168; doi: 10.1115/1.4034223

Zhang, L., Singh, V.P., 2007. Bivariate rainfall frequency distributions using Archimedean copulas. *J. Hydrol.*, 332 (1–2):93–109.

Zhang Q, Li J, Singh VP, 2011: Application of Archimedean copulas in the analysis of the precipitation extremes: effects of precipitation changes. *Theor Appl Climatol*, 107 (1–2): 255-264. doi:10.1007/s00704-011-0476-y.